



HAL
open science

Economic performance of an overplanted offshore wind farm under several commitment strategies and dynamic thermal ratings of submarine export cable

Ildar Daminov, Anne Blavette, Salvy Bourguet, H. Ben Ahmed, Thomas Soulard, Pierre Warlop

► To cite this version:

Ildar Daminov, Anne Blavette, Salvy Bourguet, H. Ben Ahmed, Thomas Soulard, et al.. Economic performance of an overplanted offshore wind farm under several commitment strategies and dynamic thermal ratings of submarine export cable. *Applied Energy*, 2023, 346, pp.121326. 10.1016/j.apenergy.2023.121326 . hal-04183205

HAL Id: hal-04183205

<https://hal.science/hal-04183205>

Submitted on 18 Aug 2023

HAL is a multi-disciplinary open access archive for the deposit and dissemination of scientific research documents, whether they are published or not. The documents may come from teaching and research institutions in France or abroad, or from public or private research centers.

L'archive ouverte pluridisciplinaire **HAL**, est destinée au dépôt et à la diffusion de documents scientifiques de niveau recherche, publiés ou non, émanant des établissements d'enseignement et de recherche français ou étrangers, des laboratoires publics ou privés.



Distributed under a Creative Commons Attribution - NonCommercial - NoDerivatives 4.0 International License

Economic performance of an overplanted offshore wind farm under several commitment strategies and dynamic thermal ratings of submarine export cable

Ildar Daminov^a, Anne Blavette^b, Salvy Bourguet^a, Hamid Ben Ahmed^b, Thomas Soulard^c, Pierre Warlop^d

^aNantes Université, Institut de Recherche en Énergie Électrique de Nantes Atlantique, IREENA, UR 4642, F-44600 Saint-Nazaire, France

^bUniversity of Rennes, ENS Rennes, CNRS, SATIE lab, avenue R. Schuman, 35170 Bruz, France

^cNantes Université, Ecole Centrale de Nantes, CNRS, LHEEA, UMR6598, F-44000 Nantes, France

^dWPD France, Nantes, France

Abstract— The overplanting of an offshore wind farm (OWF) with dynamic thermal ratings (DTR) is a promising solution for enhancing OWF performance. As the overplanted OWF generates an additional energy and DTR ensures its better transfer, the research question is if final OWF profits would be higher than associated costs. While there has been growing attention on this subject in recent years, there is still no research investigating the commitment strategies of overplanted OWFs with DTR. This paper investigates how commitment strategies may affect the economic performance of an overplanted OWF with DTR. The results show that, depending on the day-ahead commitment strategy, the annual revenue of OWFs may theoretically increase by up to 21% even without overplanting nor DTR, and by up to 204 % with overplanting and DTR. However, although commitment strategies, overplanting and DTR may significantly increase annual revenues of an OWF, its net present value (NPV) still heavily depends on market prices. In the presence of low market prices as in 2018, overplanting actually reduces the NPV of an OWF and, under the conditions considered here, keeps its NPV always negative. On the contrary, in the presence of high market prices as in 2022 or feed-in tariffs, the overplanting increases the OWF NPV. In the latter case, the NPV of the overplanted OWF is estimated between 1.5 billion and 9.5 billion euros while the discounted payback period is 3-12 years. The economic benefits of DTR for the overplanted OWF are estimated between 0.7 and 1 billion euros. The paper also shows that the optimal overplanting rate is very different whether the NPV or LCOE are considered. Finally, the paper shows that committing to the actual OWF power production (i.e. assuming a perfect power forecast) does not necessarily result in the highest revenue.

Keywords—submarine export cable, dynamic thermal rating, overplanting, imbalance, offshore wind farm

I. INTRODUCTION

A. The general context of the problem

The world's first offshore wind turbine 220 kW was built in 1990 in Nogersund, Sweden [1]. One year later (in 1991) the first offshore wind farm (OWF) of 5 MW started delivering energy from sea winds near Vindeby, Denmark [1]. At the end of 2020, the global offshore wind installed capacity has reached 35.3 GW [2]. Europe presents more than 70 % of this OWF capacity, while around 25% belongs to China. According to the DNV GL forecasts [3],[4], the total offshore wind installed capacity will continue growing worldwide, reaching 1550 GW in 2050 and generating 9 % of global electricity against 0.3 % today. The European Commission stated that no other energy technology in the past has seen such a fast development as offshore wind will grow in the next 30 years [5]. Such a rapid growth, however, requires significant investments: in Europe alone, € 800 billion will be necessary to deploy 300 GW of OWF and 40 GW of other marine energies by 2050 [5].

Although the growth of the OWF capacity is promising, the cost of this energy remains relatively high. For instance, the Levelised Cost Of Energy (LCOE) of an OWF may be 2.5 times higher than that of onshore wind farms, as shown in a British case study [6]. The difference for OWFs is mainly explained by the capital expenditures linked to foundations, the subsea transmission system (if this cost is borne by the developer) [6] as well as higher operating costs [7]. While onshore wind together with utility-scale PV [7] became the cheapest new renewable sources of electricity in 2021, in 2020, offshore wind was leading in the dynamics of cost reduction: the LCOE of offshore wind has fallen by 67 % over 8 years and continues decreasing [2]. Even though wind farms may have already reached grid parity, the costs of OWFs still need to be reduced to contribute significantly to the worldwide energy transition. Therefore, the LCOE reduction from OWFs is of paramount importance for the power industry, especially in the context of the energy transition towards decarbonized power systems.

B. Overplanting as a solution for reducing LCOE

Nowadays, a lot of research, aiming to reduce the offshore wind LCOE, is paying attention to overplanting of OWFs relative to their transmission (export) capacity [8]–[19]. Overplanting of an OWF implies installing more wind power turbines (or increasing the generator size, or even using a power boost function) than its network infrastructure can transmit in a steady state. To the best of the authors' knowledge and following [20], the concept of overplanting was proposed by Cavallo in the early 90s in a series of papers [21]–[24] on a joint operation of onshore wind farms and compressed-air storage systems [23]. At that time, Cavallo used the term “oversizing” to describe the installation of additional wind turbines relative to the associated transmission capacity [22], [23]. Further, many authors have been using different terms for the same (overplanting) concept: overcapacity [25]–[28], oversizing [29]–[36], over-installation [37]–[39] and overbuilding [29],[36],[40],[41]. Note, however, that researchers have also previously used the term “overplanting” (or a similar term) for applications differing from the one considered here, such as national generation capacity sizing for peak load management [37], [42]–[47], cross-border power import/export from

neighbouring countries [48], storage management [49]–[51]. Moreover, [47], dating back to 1977, had already used the term overplanting (relative to a national generation capacity with respect to the associated peak demand), i.e. much earlier than Cavallo proposed the oversizing of wind farms as the offshore wind industry may understand the term overplanting nowadays (i.e. relative to a transmission capacity). For the sake of clarity, it is necessary to highlight that, in this paper, we use the term overplanting relative to the network capacity of OWFs. This term is used in both the onshore and offshore wind industry, but also in the photovoltaic industry [20],[52],[53], as well as for hybrid power plants [25], [29], [38], [39], [46], [54]–[60].

Overplanting an OWF allows to increase the electricity generated annually by this farm, and thus the associated revenue, as it produces more electricity at low and medium wind speeds while requiring a curtailment only during the most energy-abundant periods (at high wind speeds). The overplanting concept is allowed in many countries on certain generating units including OWFs. For instance, in Portugal, the capacity of wind farms has been allowed to be oversized by up to 120 % of the network infrastructure capacity since 2007 [40]. In 2008, National Grid, the UK System operator (SO) issued a high-level study [61] concluding that the optimal installed capacity of OWFs could be equal to 112 % (specific for Round 3 projects) relative to their transmission capacity. Specifically for Round 3, it was proposed to install up to 1200 MW of wind capacity for a 1000 MW-rated transmission infrastructure [62]. The Netherlands and Denmark also allow overplanting based on advanced sizing techniques relying rather on the cable's maximal temperature than on the OWF's rated power (for more details see Section C).

In 2010, Boerema and MacGill [34] assessed the benefits and energy performance of oversized wind farms in Southern Australia. Specifically, they found that the additional produced energy for overplanting rates below 1.45 (i.e. 45% more installed capacity) increases in almost the same proportion as the overplanting rate. The authors conclude that, up to these overplanting rates, wind energy curtailment remains low. Moreover, they found that some wind farms may be oversized by twice of their maximal power output and still have a high capacity factor and a higher mean income per MW relative to non-oversized wind farms.

In the same year (2010), the Commission for Energy Regulation (“CER”) in Ireland allowed overplanting, as proposed by the Irish system operator (SO) [63]. This proposal was accompanied by public debates within the electric power industry. Some debate participants highlighted that 50% of transmission-connected wind farm projects and 27% of distribution-connected projects have already been over-installed by 2% and 1.8% respectively [63], as up to that moment, no power limitation existed. Hence, developers could decide to over-install wind turbines based on their studies [64]. However, in 2011, following these debates, CER assigned a cap of 5 % above the maximum export capacity (MEC) for wind farms [63]. This 5 % cap was intended to compensate for the internal losses and unavailability on the side of the wind farm.

In the same year (2011), new Irish SO studies confirmed that increasing wind farm capacities by 20 % (as in Portugal) compared to the rating of their transmission infrastructure would not affect the planning of the power system [64]. These findings, among others, allowed CER in 2014 to legally increase the cap up to 120% of the MEC. However, any MEC violations during the operation were still prohibited, therefore leading potentially to curtailment [64]. In the same year (2014), the term “overplanting” started being actively used in the literature [17], [65], [66]. Although overplanting is currently supported by system operators/regulators and already represents an emerging practice in Europe, most of the first publications on overplanting started appearing less than 15 years ago. That is why overplanting of OWFs, as a scientific topic, remains relatively new and related research is discussed in the following paragraphs.

In 2013, Harvey [32] studied the impact of oversized wind farms (by a factor of 2 relative to their transmission links) on seasonal capacity factors in Canada. Authors quantified that wind farms may increase the capacity factors in summer equal to 0.65-0.78 pu (per unit), normalized with respect to winter capacity factors, up to 0.78 - 0.81 pu if they are overplanted.

In 2014 and 2017, McInerney and Bunn [8], [19] estimated the economic benefits of offshore overplanting under different support strategies such as a feed-in tariff or FIT (implemented for instance in Germany and Spain [18]) and green certificate premium (implemented for instance in the UK and Sweden [18]). The authors showed that overplanting can be profitable under both support strategies, especially the green certificate premium. This is explained by the fact that market prices (to which premium is added) tend to be lower at higher wind speeds. Thus, the cost of curtailed wind energy, which occurs at high wind speeds (i.e. at low prices), is low. Moreover, the authors described how overplanting may positively impact investment deferral, long-term generator capacity allocations, and ancillary services. Authors found that under a FIT of £95/MWh, the optimal overplanting rate is around 8 % which ensures the net present value (NPV¹) rise of 2.3 %.

In 2015, Henderson et al [67] presented two overplanting studies performed by DONG and DNV-GL with very similar results. Specifically, the authors found that the electrical infrastructure should be sized at around 97% of the OWF capacity. This allows reducing the cost of the OWF energy by 0.5 % - 1 %.

In 2016, Getreuer et al [30] found that the optimal overcapacity of OWF is only 0.04% higher than the transmission rating. This is only 1/20th of the capacity for one additional wind turbine at 350-MW OWF. Nevertheless, the authors suggest that overplanting up to 10% may be feasible in certain situations related to the unavailability of some wind turbines or due to the combination of grid costs and energy prices. In addition, Getreuer et al [30] investigated the thermal overloading of offshore grids (the detailed discussion is presented in Section C).

¹ The net present value is the sum of the discounted cash flows normalized to their present value.

In 2017, Chen and Thiringer [18] investigated the correlation between the wind energy generation and the market price in the context of overplanting. It is demonstrated that the total profit of wind farm owners, using a fixed overplanting rate (equal to 113 % in this study), could be increased from 15% to 45.6% depending on wind-price correlations.

In 2019, Mora et al. [15],[9] integrated the uncertainty of site/technology characteristics, as well as financial constraints, into the decision process for the optimal sizing of an OWF with overplanting, modelled as a two-stage stochastic problem. The authors considered the influence of risk aversion or risk neutrality of the wind farm developer. They found that overplanting rates between 2% and 8% demonstrate better performance than the no-overplanting case. Moreover, the authors identified that wind farm availabilities and capacities, turbine sizes as well as shore distances had a significant influence on the optimal overplanting rate. At the same time, wind speeds, wake effects, inter-array cable availability as well as water depths had a still significant, but less important, influence. Further studies were conducted in Mora's doctoral thesis [68] on assessing the trade-offs between different costs in the context of overplanting while considering uncertainties and the sensitivity of overplanting to several factors (either site or technology-related). Dykes [11] demonstrated that the wake losses of overplanted OWF may be significant, and thus, they could restrict the overplanting strategies if the space for an OWF is limited.

Different regulations were also considered in 2020, where Wolter and al. [14] compared the overplanting of offshore wind farms under different regulations. Specifically, the authors studied the Danish and the UK systems and found that the UK regulation is economically more favourable to increased use of OWF network capacity. Although being less favourable, the Danish case was also profitable.

In 2021, Couto and Estanqueiro [59] investigated the feasibility of adding new wind and/or solar farms (i.e. overplanting) to existing onshore wind farms (i.e. creating a hybrid power plant) in Portugal without reinforcing the electrical network. Authors determined that adding only wind turbines to the existing wind farms (i.e. the classical view on overplanting) is less efficient because of high curtailments (up to 30 % of total production). At the same time, adding solar farms ensure only 5% of curtailments. The most interesting result is that combining solar and wind farms as additional power sources ensures the highest annual generation of an overplanted farm in comparison with the case when only one renewable technology is used for overplanting. Nevertheless, the level of curtailment for the added wind/solar units may remain up to 15%.

In 2022, Silva and Estanqueiro [69] suggested an algorithm to assess the feasibility of converting the existing wind farms into hybrid power plants. As an alternative, authors considered repowering existing wind farms without hybridization but using overplanting (only for wind turbines). It was shown that hybrid power plants ensure higher installed capacities and capacity factors, as well as better utilization of network infrastructure and lands.

In summary, all these studies have shown the positive impact of overplanting under various conditions, with an optimal overplanting rate depending on the considered hypotheses.

C. Dynamic thermal rating as a technology for better utilization of underground cables

Overplanting studies from the previous section consider the conservative assumption of static thermal rating (STR), as opposed to dynamic thermal rating (DTR), as will be discussed in this section. STR corresponds to the maximum constant current that can be applied to a cable without violating its maximum allowable temperature (usually 90°C for XLPE cables [70]) [71], [72]. However, an OWF presents a variable generation profile during its lifespan [73]. In fact, OWFs may produce at full power only 100 hours per year [74]. Moreover, due to the soil thermal inertia (depending on the cable installation, soil characteristics, burial depth along the cable route and laying configurations of the cable system), the export cable temperature may be kept far below 90°C. Hence, it is more realistic to consider dynamic thermal rating (DTR), as opposed to static thermal rating (STR). Large companies such as DNV GL [65], [66], and Danish wind energy platform Megawind [75] also indicate that the economic benefits of overplanting (around 8 %) could be significantly enhanced if the cables thermal inertias were exploited.

When DTR is considered, maximum temperature limits, as opposed to maximum current limits, are used for limiting the power flow in a transmission equipment. Note that the export cables of OWFs may represent bottlenecks for the whole offshore network infrastructure [16] when other pieces of equipment (e.g. J-tubes, transformers) are sized for a greater power rating [76]. It is also important to note that, within an export cable, several sections may represent a thermal bottleneck, such as junctions and the landing section. However, in this paper, at the first stage, we restrict our study to the subsea section excluding both the landfall section and the junctions. It may be noted that, in HVAC export cables, the conductor temperature usually represents the limiting factor for the transfer capacity rather than other constraints such as voltage swing or surge impedance [77].

Several studies have considered the combination of overplanting and DTR. In [73], authors showed that it is possible to reduce the cross section of an export cable by 25 % without violating the temperature constraints if both the actual power profile of the OWF and the cable thermal inertia are considered. Danish system operator Energinet used this technique for sizing the export cables at 400 MW for OWF "Horns Reef 3" in Denmark [73]. Dutch operator TenneT also allows overplanting and the exploitation of thermal inertia [16]. More specifically, TenneT permits operating the export cable above its steady state power limit (i.e. its STR), as long as the power flow remains below a certain limit and if the cable temperature does not exceed a pre-defined limit. The details on how TenneT sizes its export cables considering DTR are given in [78]. In practice, in OWF zone Borssele in the Netherlands, 8% to 9 % overplanting is allowed [15], [10],[79]. The network infrastructure capacity for sites I, II and IV of the Borssele OWF is equal to 350 MW and 330 MW for site III accordingly [79]. At the same time, the maximum allowed OWF installed capacities for these given sites are 380 MW and 360 MW respectively, thus corresponding to 30 MW above the network capacity in each case [15]. In [80], the overplanting for the Hollandse Kust OWF in the Netherlands is considered, and the same overplanting rates as for Borssele OWF (350MW+30 MW) are used for sites I-IV. Another study [81] exists for Hollandse Kust (Site V) having 760 MW of wind capacity versus 700 MW of guaranteed transmission capacity.

Few studies exist on DTR for offshore grids. For instance, Getreuer et al [30] investigated the thermal overloading of meshed offshore grids in 2016, including an oversized OWF (by 4%). They concluded that during the maintenance periods of the meshed network, short-term overloading (in terms of temperature) insignificantly reduces energy curtailments relative to non-overplanted OWF: the difference is around 0.1%-1.4%. However, this effect on energy curtailments will be reassessed in the following studies considering overplanting rates higher than 4%. Pilgrim and Kelly [74] suggested a method to find the optimal number of wind turbines considering the DTR of the submarine export cable. They considered the minimization of the cable contribution to the LCOE and showed that the LCOE could be reduced by £1/MWh (the generation costs of OWF are assumed as £70/MWh) while increasing the wind farm production by 19%. This is equivalent to reducing the cable CAPEX by 14 %. In 2020, Hernandez Colin presented a doctoral thesis on day-ahead (DA) management including probabilistic algorithms considering DTR [82], [13]. In 2021, another doctoral thesis by Syed Hamza Kazmi addressed the DTR of offshore infrastructure including both cables and transformers [83]. Specifically, the thesis defines the thermal bottlenecks of the OWF infrastructure and solves the operational problem (for onshore lines and transformers only [84], [85]) and the integrated sizing-operational optimization problem under uncertainties (for export cables and transformers) [86],[87].

D. Day-ahead planning and paper goals

As mentioned earlier, DA planning considering the combination of overplanting and DTR was analyzed in Hernandez Colin [82]. This research considered a revenue, based on energy prices fixed at least the day before, and a curtailment strategy. However, as forecasts are inherently imperfect, there may be significant mismatches between the power profile forecast by the energy supplier and the farm's actual power profile. These discrepancies may be compensated by the TSO through balancing reserves. On a financial level, the Balance Responsible Party (BRP) in charge of a given Balance Perimeter, to which the energy supplier belongs, is therefore either paid by the TSO for an excess of energy compared to the production forecast or pays the TSO in case of an energy deficit. Recently, offshore wind farm Borkum Riffgrund 1 started supplying secondary reserves to the German grid [88]. One of the goals of this paper is therefore to consider the additional revenue/penalties linked with imbalances when considering a DA power commitment strategy in an overplanted OWF where DTR is allowed.

DA commitment strategies are based on forecasts of OWF power output among others [89]. These forecasts are usually provided to the energy supplier in the form of several quantiles. These quantiles are expressed as a daily profile where each hourly quantile "PX" refers to the level of power that the wind production has (100%-X%) chance of exceeding. For instance, the P50 quantile represents a forecasted power level which could be exceeded with a 50% chance (100%-50%). Quantiles may be used to generate scenarios with which stochastic optimization studies can be performed, therefore producing optimal stochastic commitment strategies. However, developing these scenarios requires considering some hypotheses regarding the temporal structure of the wind power profile. Usual models consider statistic time-series models such as ARMA, ARIMA, etc. However, they do not perform well to capture the volatility of wind power on timescales of tens of minutes [90]. This constitutes an issue as imbalance settlement periods are soon to be harmonized at a shorter timescale of 15 min in Europe [91], despite quantiles being provided on an hourly basis. Hence, energy suppliers tend to continue using a relatively simple commitment strategy based on the 50% quantile called the P50. Another goal of this paper is therefore to consider several commitment strategies, which will be compared with the usual P50 strategy.

In our paper, both the DA prices and the imbalance prices are considered as known in advance while the wind power production remains uncertain. Hence, these cases are theoretical, as DA prices are known after the market clearing (i.e. after the commitment has been done) while imbalance prices are known *a posteriori*, but they allow to provide an upper boundary on the maximum revenue that could be expected. DA price forecasting has been studied in many studies [92]. As renewables are becoming the main cause of imbalances in many power systems, such imbalances may become more and more predictable at different lead times [93]. Research on imbalance volume and price forecasts is emerging, as there may indeed be some significant benefits for the energy market actors to exploit imbalances [94], although this may be worrying for grid operators [93], [95]–[97].

E. Contributions

The main contributions of this paper are as follows:

1. Benefits of overplanted OWF with DTR are quantified for the case when revenue/cost from both DA energy sales and imbalances are considered.
2. The "business as usual" P50 commitment strategy is compared with other commitment strategies in the context of overplanting, and its combination with DTR.
3. Economic metrics such as NPV, LCOE and discounted payback periods are estimated for low and high market prices.
4. The economic benefits of DTR for export cables over the lifetime of an overplanted OWF are estimated.

The paper is organized as follows: Section II details the models and data used in our paper, Section III presents the methodology and Section IV describes the results and discussion. Finally, Section V concludes our research.

II. MODELLING AND INPUT DATA

In our case study, the OWF is connected through one submarine cable to an onshore substation (see Figure 1). Other elements e.g. offshore and onshore power transformers, J-tubes, etc. are assumed to be sized at a sufficient rating so that they do not represent a thermal bottleneck. This approach is similar to the one investigated by TenneT [12] for a 350 MW OWF presenting

30 MW of possible overplanting (i.e. resulting in a maximum rated capacity of 380 MW) where the J-tubes (having particularly low thermal inertia levels) [16], as well as the transformers [98], are sized for the maximum rated capacity or above. Hence, the export cable (including its landfall and submarine sections) may represent the bottleneck of the network infrastructure. In our study, only the submarine part of the HVAC export cable is considered. The cable junctions have not been considered at this stage due to the absence of available models although they present lower thermal inertia than the rest of the submarine cable.

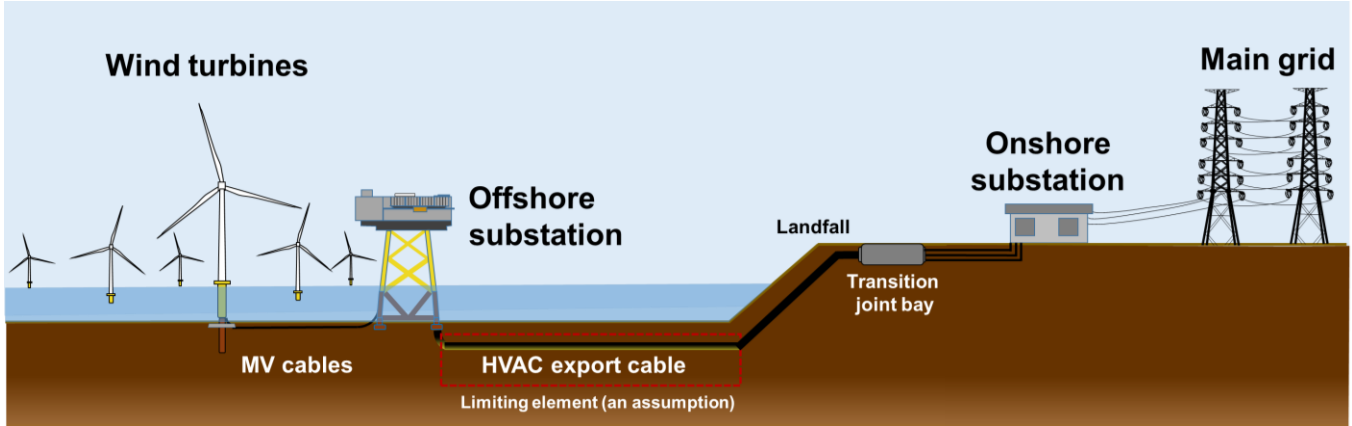


Figure 1 Illustration of the electrical infrastructure of an OWF

In this paper, a HVAC 3-core submarine cable is considered. Its cross-section is equal to 1000 mm², its rated power to 339 MVA, and its rated voltage to 225 kV. Its geometry and materials characteristics are provided by the French transmission system operator RTE. Note that throughout this paper, we always use the same export cable (339 MVA). Therefore, the OWF installed capacity will change as a function of the overplanting rate, but the export cable capacity remains always the same (339 MVA). Figure 2 shows the cross section of a similar export cable and its 3D view, both created using the site Cableizer [99]. In the first stage, we assume a power factor equal to one. It is important to note that cables generate reactive power, therefore potentially requiring reactive power compensation devices, while energy producers are also legally required to provide reactive power absorption/supply services. Hence, the transfer of active power through the considered cable can never be equal to the apparent rated power of the cable, which represents a limitation of this study. Future research will consider this aspect.



Figure 2 Cross-section and 3D view of a cable similar to the one used in our paper. Reproduced with the permission of Cableizer

A. Mathematical formulation

The problem considered here consists in maximizing the annual revenue obtained from the OWF. As will be described later in this section, most of the strategies studied in this paper are based on heuristics, but a daily optimization problem is also considered (more specifically the optimal power profile strategy $P_{\text{OptimProfile}}$ which will be described later). This daily optimization problem is expressed as follows:

$$P_{\text{plan}(t)}^{\max} C_E(d) = \Delta t \cdot \sum_{t=0}^{t=23h45} [P_{\text{plan}}(t) \cdot c_{D-1}(t) - [\max(0, P_{\text{plan}}(t) - P_{\text{actual}}(t)) \cdot c_{B-}(t) + [\max(0, P_{\text{actual}}(t) - P_{\text{plan}}(t)) \cdot c_{B+}(t)] \quad (1)$$

Subject to

$$I_{\text{actual}}(t) = \frac{P_{\text{actual}}(t)}{\sqrt{3} \cdot V \cdot \cos\varphi} \quad (2)$$

$$(I_{actual}(t) \leq I_{adm} = 871 A \text{ (if the current constraint is considered, i.e. STR case)})$$

or

$$T(t) \leq T_{max} = 90^\circ C \text{ (if the temperature constraint is considered, i.e. DTR case)}$$

$$T(t) = f(I_{actual}(t_0, \dots, t))$$

Where Δt – time step of 15 minutes

$C_E(d)$ – OWF revenue for the day d

$P_{plan}(t), P_{actual}(t)$ – the OWF committed and actual power output at time t

$c_{D-1}(t)$ – DA price at time t

$c_{B-}(t), c_{B+}(t)$ – imbalance prices for under-production and over-production regulation

I_{actual} – actual current injected into the export cable from the OWF (after the step-up transformer at the offshore substation)

V – nominal voltage of the export cable. We assume that the voltage is constant and equal to 225 kV.

$\cos\phi$ – power factor. We assume that the power factor is equal to 1 which corresponds to the requirements for OWF on their reactive power capabilities in a normal operation (0 MVar) [98]. This is of course an assumption since different components in offshore grids may be producers and consumers of reactive power, especially underground cables, thus needing potentially reactive power compensation devices [100]. Considering a unity power factor is therefore optimistic, and a more refined assumption will be analyzed in future work.

I_{adm} – admissible current of the export cable per IEC standard 60287 (steady-state rating)

$f(I_{actual}(t_0, \dots, t))$ – thermal model of the export cable based on IEC standard 60853-2

$T(t)$ – export cable temperature

T_{max} – maximum allowable temperature of the export cable

Note that we limit the actual current $I_{actual}(t)$ only at the delivery time. This means that day before (d-1), the commitment can be done for any power profile, provided that it is below the installed OWF installed capacity. This assumption represents the situation where a TSO would curtail the wind power output in real time if the cable limits are exceeded (90 °C for the DTR case or 871 A for the STR case). The curtailment algorithm, simulating this TSO behaviour, is given in Section III.

B. OWF generation forecast and actual production

In this article, we use power measurements of real Belgian OWFs and the corresponding forecasts in the form of quantiles (P90, P50 and P10) to model the OWF power profile. This data is provided by Belgian system operator Elia [101]. In general, the number in the quantile abbreviation, as 50 in P50, means how often the actual power output of OWF is expected to be below its forecasted power output (see Figure 3 for the performance of Elia’s forecast data). Thus, P10 would be prone to underestimate the actual power output whereas P90 would be prone to overestimate it. The P50 quantile is balanced as 50% of the time the actual power would be below P50 and another 50 % of the time the actual power would be above the P50 forecast.

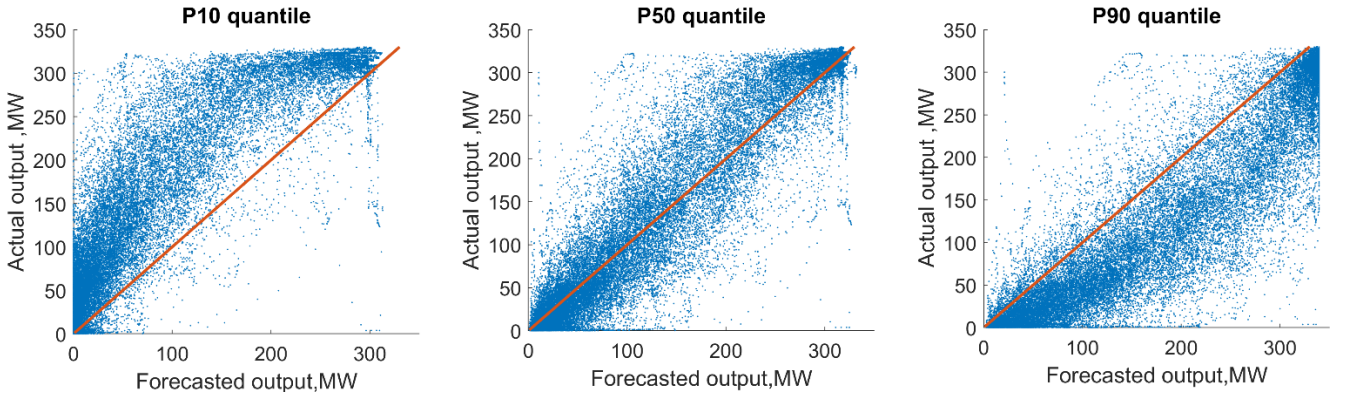


Figure 3 OWF forecast performance for quantiles: P10, P50 and P90. Source: Elia [101]

Figure 4 shows the actual production of the OWFs connected to Elia’s network, as well as the corresponding quantile profiles in per units. To generate a power profile in MW for the given overplanting rate (for both the measured and the forecast data), their initial power profile in pu is multiplied by the targeted installed capacity: from 339 MW up to 679 MW. It must be noted that this proportional method is approximate, as it does not consider any changes in the power profile shape due to upscaling/downscaling (no increased power smoothing due to the aggregation effect in a larger farm, wake losses variation, etc.). However, this was deemed sufficient for the purpose of the considered study.

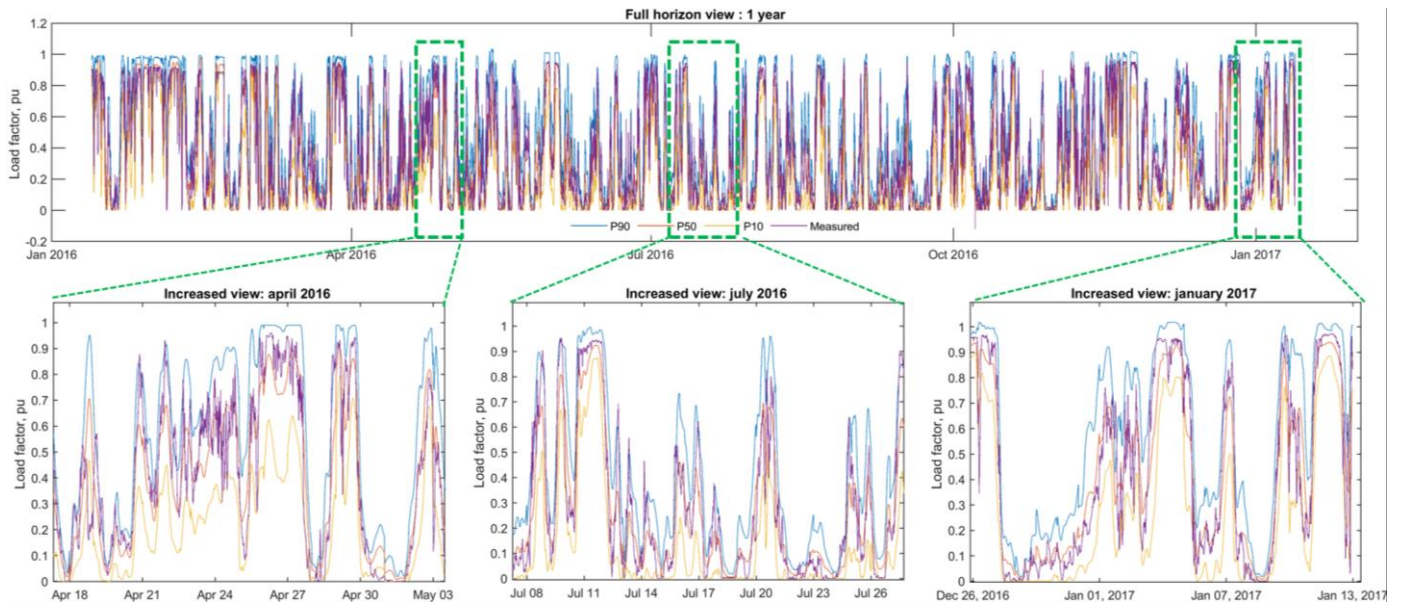


Figure 4 Power generation forecasts and actual measurements of the OWFs connected to Elia's network

C. Energy prices: day-ahead prices and imbalances prices

The electricity generated by the OWF is considered here to be sold on the DA market and does not include any subsidy. It is also assumed that mismatches between the commitment and the actual production are purchased/remunerated at the imbalance prices. The ENTSO-E datasets for the period of January 13, 2018 – January 12, 2019, in France were used for both energy prices (both DA and imbalances) [102], [103]. It is important to note that the wind production and price data are selected from two different countries (Belgium and France respectively), as no offshore wind farm was being operated in France (which our study targeted) when this research work was carried out. Although a price difference may be observed between France and Belgium, it was assumed that offshore wind production is still sufficiently small not to influence the market prices. Hence, it was assumed reasonable to combine these two sources of data in our study. Note also that this period of market prices does not correspond to the period of the wind production and forecasts time series (13 January 2016 - 13 January 2017) due to a lack of reliable imbalance prices for this period. Nevertheless, it was assumed that the decoupling of power and price time series should not affect the study.

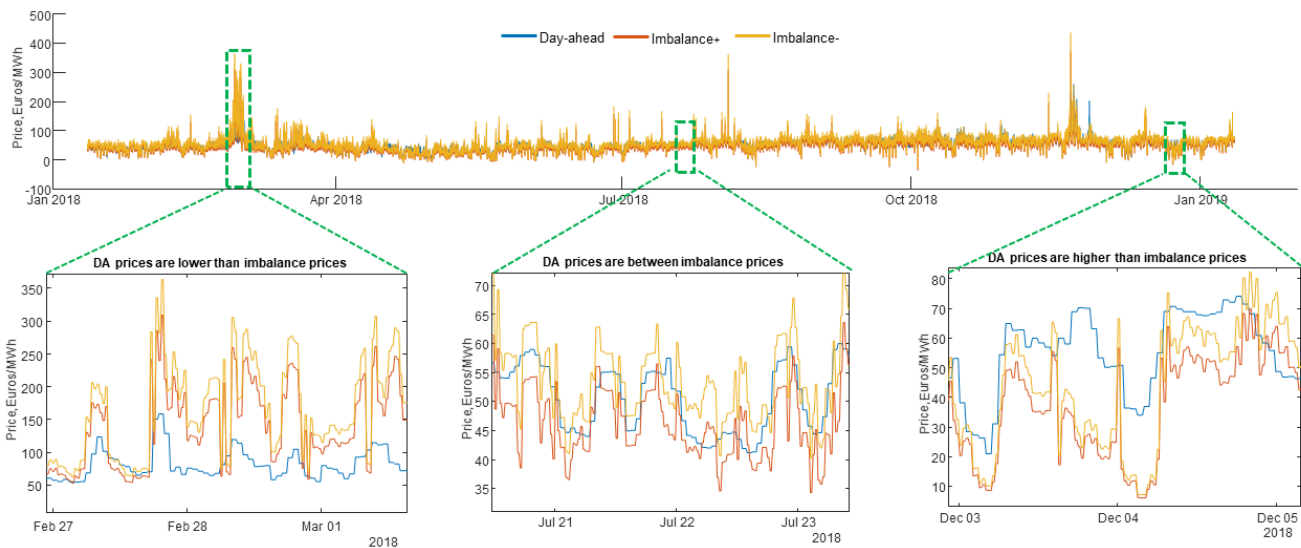


Figure 5 Market prices in France and different situations where the DA price may be higher, in-between or less than the imbalance prices.

It is interesting to note that DA prices may be higher or less than the imbalance prices, as shown in Figure 5. This means that selling energy as an imbalance, rather than on the DA market, may sometimes be more beneficial in terms of the revenue. Knowledge of the future energy prices (DA and imbalance) is of course limited, as DA prices can only be known after the market clearing (i.e. after a commitment is done) while the imbalance prices are known *a posteriori* after the imbalance settlement period (soon to be harmonized to 15 min in Europe) and can therefore only be estimated before real time. However, the DA price can be forecasted to some extent and there has been recently a growing interest in imbalance price and volume forecasting, as mentioned in the introduction. Hence, in this paper, we assume that imbalance prices are known perfectly in

advance to allow the choice between the DA market and the imbalance regime. This represents a theoretical case which allows us defining the upper boundary for the maximum revenue than can be obtained.

D. Thermal modelling of the export cable and validation

For the type of an export cable given in Section II, the maximum allowed temperature is equal to 90°C . We assumed that curtailment of wind power is applied as soon as the temperature reaches this value. However, temperature monitoring devices may present a coarser precision of a few degrees. This may require to curtail a wind power at a few degrees less than 90°C (a sensitivity analysis was carried out in this perspective in this paper). The electro-thermal model used in this paper was developed in MATLAB based on IEC standard 60853-2 [104]. The IEC 60853-2 model is based on a two-cell RC equivalent circuit which is shown in Figure 6. The soil temperature is assumed to be always equal to 18°C and the cable burial depth is 1.87 meters.

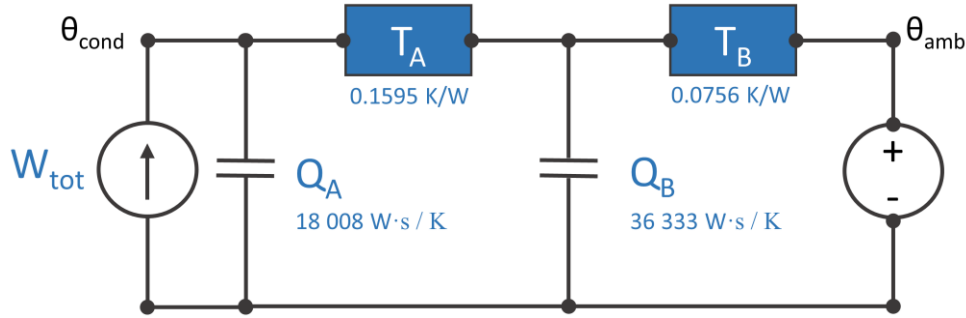


Figure 6 Equivalent thermal circuit with two cells and corresponding values

As the IEC standard presents a sophisticated procedure with some ambiguities, we decided to provide the details of our model in supplementary material to be published soon on the project webpage [105]. In this paper, however, we show only the validation results for this thermal model. Specifically, the thermal model was developed in MATLAB and then validated against temperature profiles provided by RTE (see Figure 7). As a result of these simulations, the difference in temperature estimation between the MATLAB and reference data converges to zero, and never exceeds 2°C . Hence, it is assumed that our MATLAB model is sufficiently precise at this stage for the simulations presented in this paper. Note, however, that the MATLAB model provided in open access [106] is a little bit different from the MATLAB model used in the simulations shown here, as the latter was additionally calibrated thanks to confidential data. Nevertheless, the only difference for the open-access model consists in several parameters whose absence would still result in similar temperature calculations as for a calibrated model.

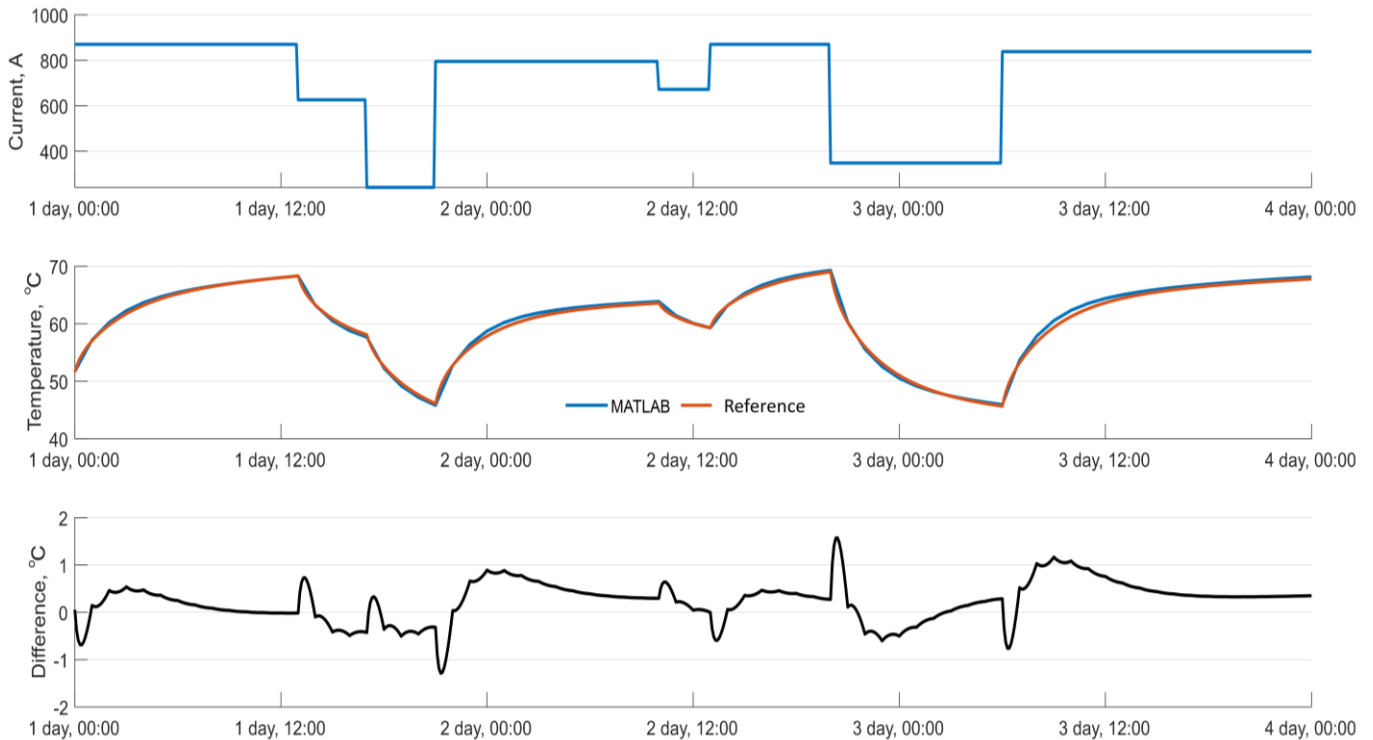


Figure 7 Validation of the thermal model against reference temperature profiles

III. METHODOLOGY

In this section, we present the methodology used to estimate the annual revenue generated from an OWF as a function of several commitment strategies combined or not with DTR. The methodology considering CAPEX and OPEX is also presented in this section.

A. Case studies

Four case studies are considered in this paper. Each case study estimates the influence of a given aspect or their combination on the annual revenue. Their characteristics are presented in Table 1.

Table 1 Characteristics of the 4 case studies considered in this paper

Case study #	Commitment strategy	Overplanting rate, pu	Cable limit	Aspect studied in the case study
1	P50 quantile	1	Current 871 A	Reference (Business as usual)
2	Five commitment strategies	1	Current 871 A	Commitment strategy
3		1-2	Current 871 A	Commitment strategy + Overplanting
4		1-2	Temperature 90 °C	Commitment strategy + Overplanting + DTR

Five commitment strategies are considered: the business-as-usual strategy (referred to as P50), the fixed quantile strategy ($P_{\text{FixedQuantile}}$), the actual power profile strategy (P_{actual}), the variable quantile strategy ($P_{\text{VarQuantile}}$), the optimum power profile strategy ($P_{\text{OptimProfile}}$). Table 2 shows the description of each strategy used in this paper.

Table 2 Description of the different commitment strategies

Symbol	Description of strategy
P50	This is a business-as-usual strategy and it is used as a reference in this paper. The idea of the P50 strategy is that the power profile commitment corresponds to the P50 quantile. Under the P50 strategy, we assume that the P50 quantile is selected as the power commitment every day of the year. In other words, the P50 remains always the commitment strategy whether or not it may violate the cable limits, especially at high overplanting rates. Any actual violation of the cable limits is assumed to be mitigated thanks to curtailments close to the delivery time. Therefore, any deviation from the committed power profile would be remunerated (or penalized) at the current imbalance price. This is assumed to be representative of a case where no thermal model is shared by the transmission system operator, for instance for commercial confidentiality reasons.
$P_{\text{FixedQuantile}}$	This strategy is very close to the P50 strategy, but instead of using the P50 quantile, another quantile is retained that maximizes the annual revenue over the year considered. Again, this quantile is used for the power commitment profile for every day of the year. In this paper, we calculated exhaustively the annual revenue for all 99 quantiles: P01...P99. Note also that we assume that no cable constraints are applied on the committed power profile (except that it should be lower than the OWF installed capacity). In other words, the submitted power profile may violate the cable limits in the case of an overplanted OWF, but this again is assumed to be mitigated through curtailment close to the delivery stage, if necessary (the algorithm of such power curtailment is given in the next section).
P_{actual}	This strategy represents the ideal situation: the committed profile matches the power profile which would actually occur on the next day. In this case, the cable constraints (either in terms of current or in terms of temperature) are considered. This represents the hypothetical situation where generation forecasts are perfect (i.e. with an accuracy of 100 %), and a sufficient level of information (e.g. on the cable thermal model) is shared between the different actors (transmission system operator, OWF manager, etc.), with a sufficient lead time, so that the commitment can be done on the actual power profile (considering cable constraints). This case is theoretical but this strategy allows to provide an upper boundary on the maximum revenue obtained from the DA market. Note that in this case, no quantiles are considered because the actual power profile may shift from one quantile to another and even not follow them at all. Thus, this strategy should neither be considered as quantile-based as the two previous ones, nor as the next strategy. The P_{actual} strategy also represents the situation when the revenue does not include any imbalance cost/rewards as the submitted power profile is equal to the actual power profile. Hence, the revenue of such a strategy would depend only on the revenue from the DA market whereas the revenue generated from all other strategies presented in this table may incorporate imbalance costs/rewards.
$P_{\text{VarQuantile}}$	This strategy is quantile-based as the previous P50 and $P_{\text{FixedQuantile}}$ strategies. However, these two strategies assumed that the same quantile is used each day over the whole year. In contrast, $P_{\text{VarQuantile}}$ assumes that the optimal quantile is selected (ensuring the highest revenue on a daily basis).
$P_{\text{OptimProfile}}$	This strategy is not quantile-based and not related to any power profile as in the case of the actual power profile strategy (P_{actual}) strategy. Thus, the main difference of this strategy is that it allows committing to any power profile on the DA market. However, under such strategy, an optimization problem must be solved to choose the optimal power profile shape that maximizes the daily revenue, while not exceeding the OWF installed capacity. Moreover, the strategy (in a similar way to the quantile-based strategies) does not imply possible violations of

the cable limits. In this case, again, curtailment would be assumed to occur close to the delivery time and the resulting energy deficit would be paid as an imbalance. This strategy generates the highest theoretical revenue, assuming perfect forecasts on both wind power production and energy prices. Again, this case is theoretical, and we do not try to propose the best strategy under uncertainty, as our goal is to quantify the upper boundary for revenue from the OWF.

B. Block scheme

The general flowchart of simulations is presented in Figure 8. The block scheme consists of three main stages:

1. Data preparation. At this stage, we convert the initial power profiles from Elia's site (in per units) into MW values for the given overplanting rate. As it is mentioned in Section II, this is done by multiplying each per-unit power profile by the OWF installed capacity corresponding to the selected overplanting rate. This stage is essential because the capacity of OWF changes as a function of overplanting rate (from 339 MW to 679 MW) but the capacity of the cable remains the same (339 MVA).
2. Day-by-day simulations to calculate the OWF's revenue. In this stage, we go through each day, day by day, until the last (365th) day is simulated. In each iteration, we calculate the OWF revenue as a function of the different commitment strategies and cable limits (current or temperature). Here, we also calculate the actual OWF power profile which may require power curtailment. The curtailment algorithm, simulating the TSO requests and wind farm manager actions, is given below in pseudo-code:

Algorithm for power curtailment

1. Input: OWF daily current profile (15-min resolution):

$I_{\text{cable}}(t)$ where $t = 1 : 96$

2. If a current limit is applied (871 A) (static thermal rating case)

Check if $I_{\text{cable}}(t) > 871$ A:

while $I_{\text{cable}}(t) > 871$ A

(a) Find the time instants when the current exceeds its limit:

$\text{idx_current} = \text{find}(I_{\text{cable}}(t) > 871 \text{ A})$

(b) Reduce I_{cable} when it exceeds its limit for the first time:

$I_{\text{cable}}(\text{idx_current}) = 871 \text{ A}$

end

3. If a temperature limit is applied (90°C) (dynamic thermal rating case)

Check if $I_{\text{cable}}(t) > 871$ A:

Calculate the daily temperature profile T_{cable} of the export cable:

$[T_{\text{cable}}(t)] = f(I_{\text{cable}}(t_0), \dots, t)$

Check if $T_{\text{cable}}(t) > 90$ °C:

while $T_{\text{cable}}(t) > 90$ °C

(a) Find the instants when the temperature exceeds its limit:

$\text{idx_temperature} = \text{find}(T_{\text{cable}}(t) > 90)$;

(b) Reduce I_{cable} when T exceeds its limit for the first time:

$I_{\text{cable}}(\text{idx_temperature}(1)) = I_{\text{cable}}(\text{idx_temperature}(1)) \times (1 - \Delta)$, where $\Delta = 0.01$

(c) Calculate the daily temperature profile of the export cable after the curtailment

$[T_{\text{cable}}(t)] = f(I_{\text{cable}}(t))$

end

4. Return the current profile, respecting the cable current or temperature constraint

3. Post-processing of the obtained results. Once all daily simulations are performed, we calculate the annual revenue corresponding to the different commitment strategies.

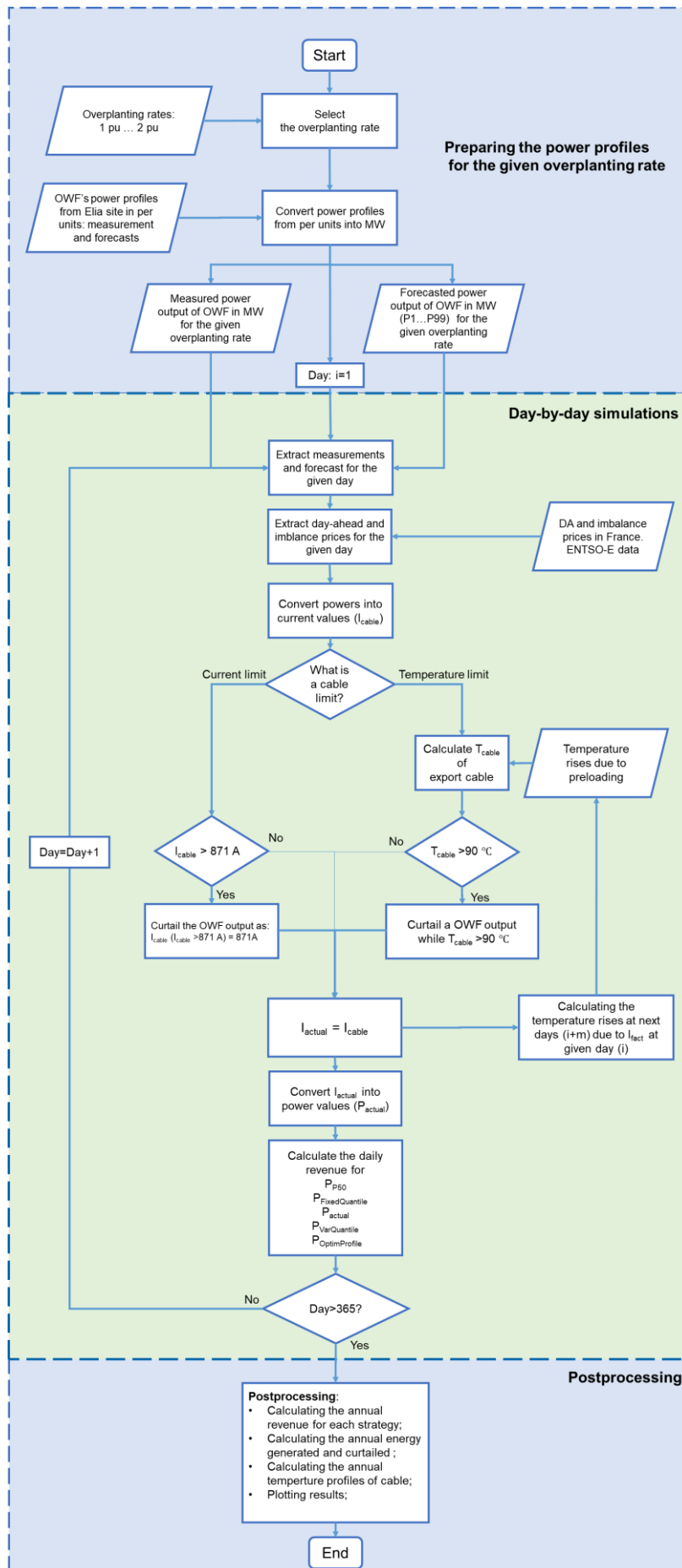


Figure 8 Block scheme for performing the simulations

C. Methodology for the analysis of LCOE, NPV and payback periods

In this section, we describe the data and the methodology used for the analysis of LCOE, NPV and discounted payback periods. To conduct such analysis, we use data on capital and operational expenditures for OWF from CATAPULT [107]. The CATAPULT data [107] represents CAPEX and OPEX broken down into equipment categories which are especially useful in our case as it allows us to separate costs of export cables (130 000 £/MW) from other balance of plant costs (array cables, power transformers among others). According to provided CATAPULT data [107], the CAPEX and OPEX change linearly as a function of overplanting rate (see Figure 9).

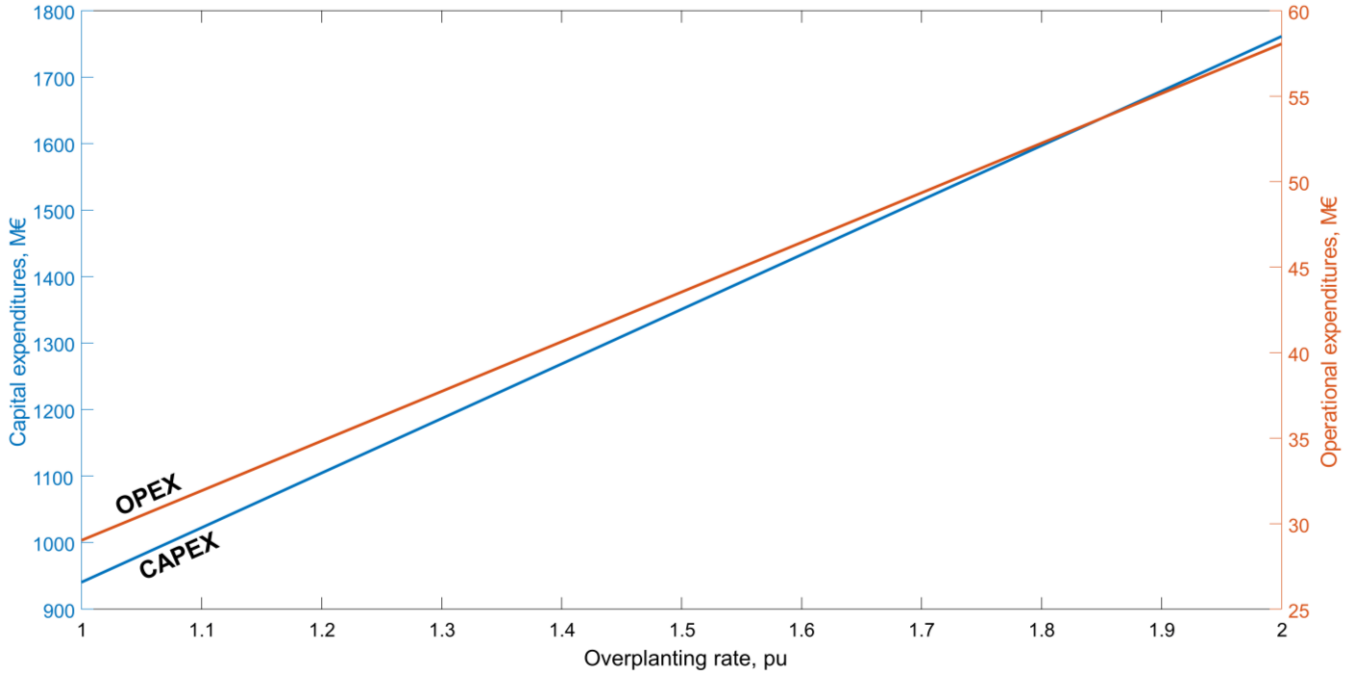


Figure 9 CAPEX and OPEX of OWF as a function of the overplanting rate

For the calculation of LCOE, we use the formula representing the ratio between total discounted costs and discounted energy production:

$$LCOE = \frac{CAPEX + \sum_{t=1}^{27} \frac{OPEX}{(1+d)^t}}{\sum_{t=1}^{27} \frac{E(t)}{(1+d)^t}} \quad (5)$$

Where d – the discount rate of 2.5 %; $E(t)$ – generated annual energy, MWh; t – studied year (from 1 to 27)

For the calculation of NPV, we use the following formula:

$$NPV = -CAPEX + \sum_{t=1}^{27} \frac{Cash\ flow(t)}{(1+d)^t} \quad (6)$$

Where $Cash\ flow(t)$ – the cash flow at the year t , representing the difference between the annual revenue and OPEX. Note that the nominal cash flow $Cash\ flow(t)$ in the numerator is assumed to be the same for all years t .

for each commitment strategy:

for each overplanting rate

set $t=0$ and Discounted revenue=0

calculate CF i.e. cash flow for a given strategy and overplanting rate

while CAPEX > Discounted revenue(t)

$t=t+1$

if Discounted Revenue ($t-1$) = Discounted Revenue (t)

$t=inf$ and break

else

Discounted revenue (t) = Discount revenue ($t-1$)+CF/(1+d) ^{t}

end

end

end

end

IV. RESULTS AND DISCUSSION

A. Impact of the commitment strategy on the annual revenue (Case study 2)

In section A, different commitment strategies are compared for a non-overplanted OWF (339 MW). Thus, no curtailment is required and therefore cable limits are based on the STR. Figure 10 shows the annual revenue for different commitment strategies, compared to the “business as usual” commitment strategy where the P50 quantile is used (the grey bar).

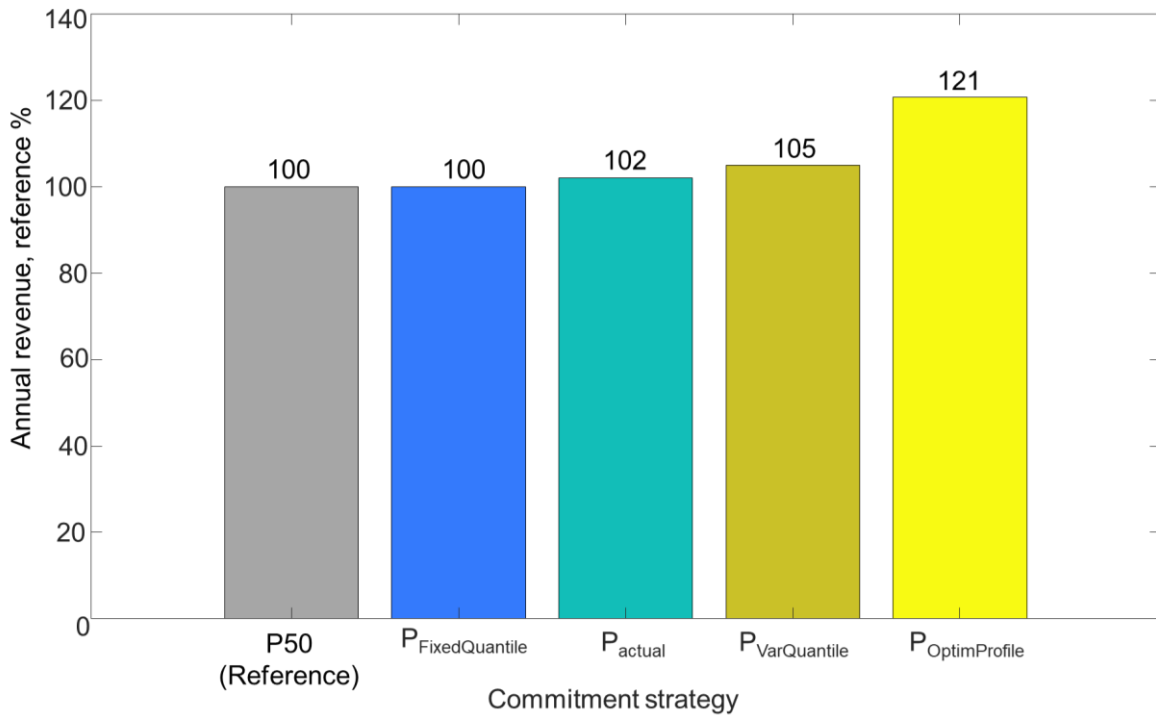


Figure 10 Impact of commitment strategies on the annual revenue of a non-overplanted OWF: Case 2

The blue bar, representing the fixed quantile strategy (“ $P_{\text{FixedQuantile}}$ ”), shows that there is no significant additional revenue from using the best-fixed quantile, which is equal to P55 here. In general, the function of fixed quantiles is relatively flat over a large quantile range, as shown in Figure 11. Note that the difference between the highest and lowest value of the curve is around 4% for non-overplanted OWF. For overplanted OWFs, as we will see later in Figure 17, this difference may increase up to 6% (for an overplanting rate equal to 2 pu). Nevertheless, this still shows the relative flatness of the considered problem within a large quantile range.

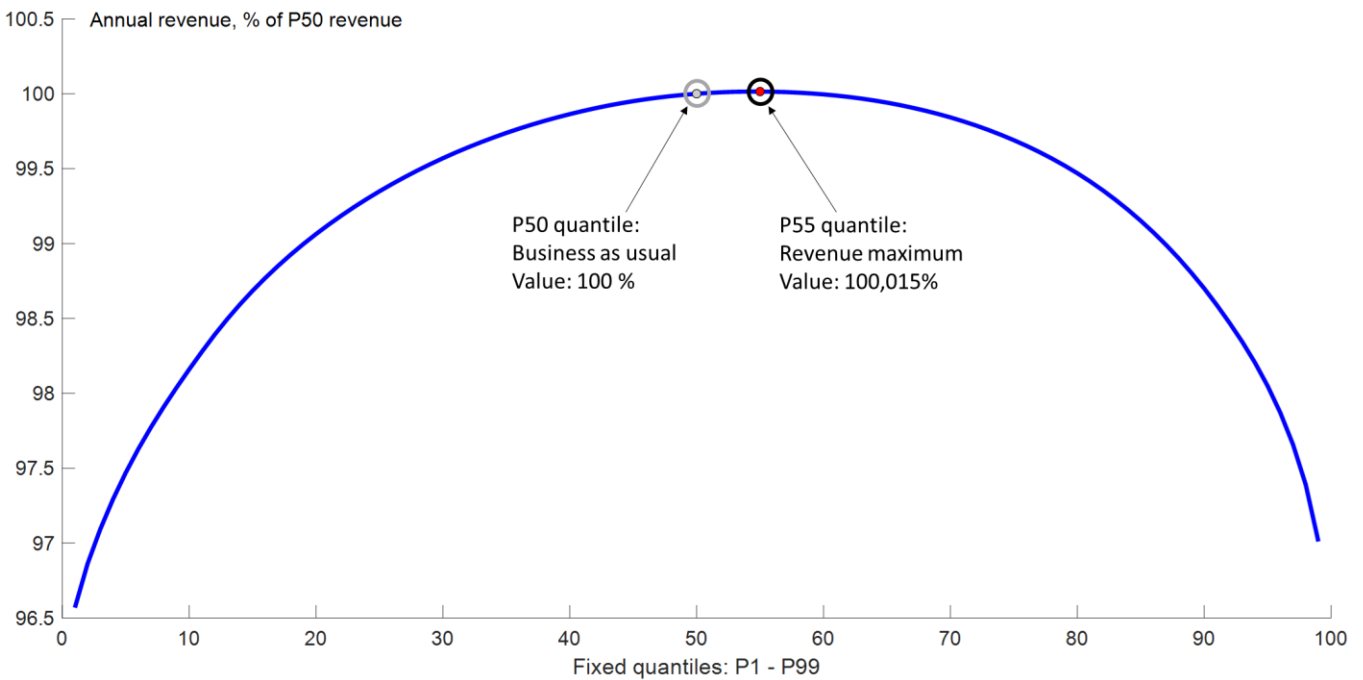


Figure 11 Annual revenue as a function of fixed quantile for a non-overplanted OWF

This revenue flatness can be explained by the symmetrical dispersion of prices difference against power mismatches (see Figure 12). As a result, this leads to close average values for the imbalance prices and the DA prices. On the one hand, the deficit in energy leads to the revenue paid at the DA price for the committed volume of energy minus the cost paid at the negative imbalance price (imbalance-) for the difference between the committed and the actual power production. On the other hand, an excess of energy leads to the revenue paid on a smaller committed volume of energy plus the revenue paid at the positive imbalance price (imbalance+) for the rest of the produced energy. However, the costs/rewards are similar on a yearly average, regardless of whether the energy is sold on the day-ahead market or at the imbalance price. Hence, the annual revenue is quite insensitive to the selected quantile when a fixed quantile strategy is used.

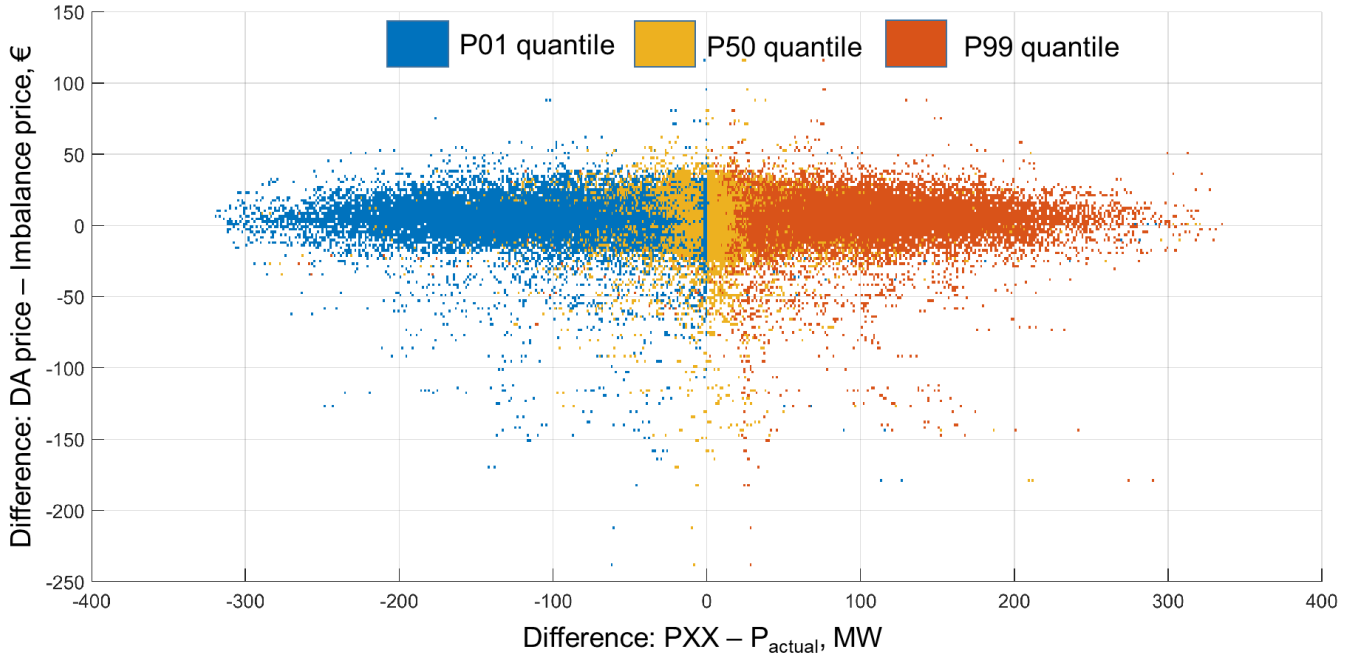


Figure 12 Scatter plot showing the price and power differences for a non-overplanted OWF

Going back to Figure 10, it shows that the P_{actual} strategy (the cyan bar) for which the commitment is made on the actual OWF production, i.e. in the ideal case where the forecast is perfect, would help to gain only 2% of additional revenue. In such a case, all the energy produced would be sold at the DA price only. This implies that this strategy does not consider exploiting imbalances, which can sometimes be paid at higher prices than the DA prices. Figure 13 shows the positive imbalance prices (imbalance+) plotted as a function of the DA prices at the same instant. The positive imbalance price (referred to as imbalance+ in this paper) corresponds to the price at which the excess of energy would be sold.

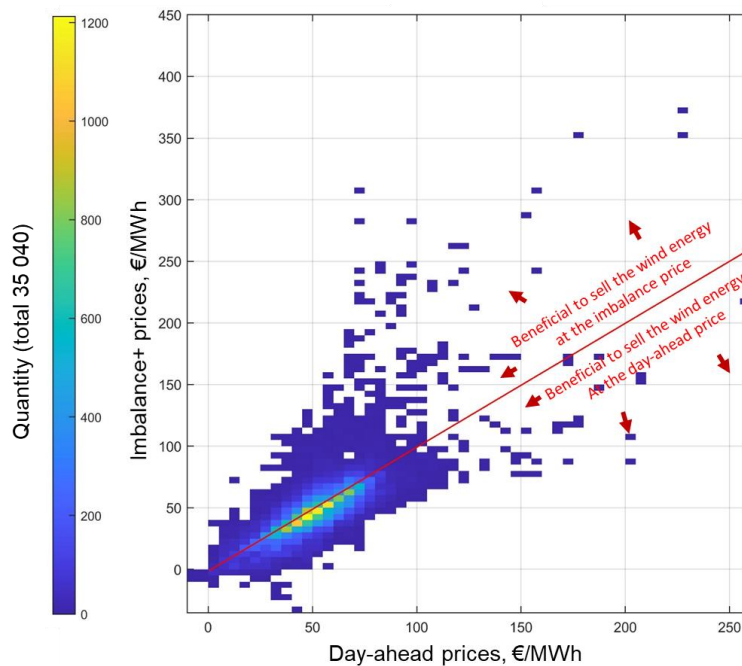


Figure 13 Imbalance+ prices versus DA prices during the considered period in France

All points above the red line show market conditions when it is possible to sell wind energy at a higher imbalance+ price (y-axis) than the DA prices (x-axis). This situation happens 27% of the year and it would be more beneficial, in these cases, to sell energy at the imbalance prices rather than at the day-ahead prices. However, as the “actual” strategy avoids any mismatch between the committed and actual power generation, then it does not allow to sell an excess of wind energy at higher imbalance+ prices when it is possible to do that. Thus, the final gain remains low despite the perfect knowledge of the OWF’s actual production. However, it confirms the relevance of using a fixed quantile strategy (the P50 or any other quantile around it) as similar gains are expected if the wind production forecast is perfect. This suggests that improving production forecasts only, and not in combination with an imbalance price forecast, may not lead to a significant increase in revenue.

The green bar in Figure 10, corresponding to the variable quantile strategy (“ $P_{VarQuantile}$ ”) leads to a more significant growth in revenues – 5 % in comparison to the P50 strategy. Graphically, this strategy includes some of the points above the red line in Figure 13 which represent the days when the revenue can be increased by selling energy at imbalance prices higher than the DA prices. Considering such days, the additional revenue may be doubled in comparison with the actual power strategy (from 2% to 5% with respect to the P50 strategy). This shows the benefit that could be gained from exploiting imbalances, even though the commitment profile is restricted to a quantile profile which is based on forecasts.

Finally, the yellow bar in Figure 10, corresponding to the optimal profile $P_{OptimProfile}$ strategy, shows the highest margin of additional revenue (21 %). In this case, full exploitation of the DA and imbalance prices is allowed as there is no restriction on the power commitment profile that can be adopted, except that it cannot exceed the maximum rated power of the farm. For instance, Figure 14 shows the situation (bottom subplot) on February 29, 2018, in France when imbalance prices were mostly higher than the DA prices. The top subplot shows the power profiles of the OWF for $P_{OptimProfile}$ strategy and other previous strategies for information.

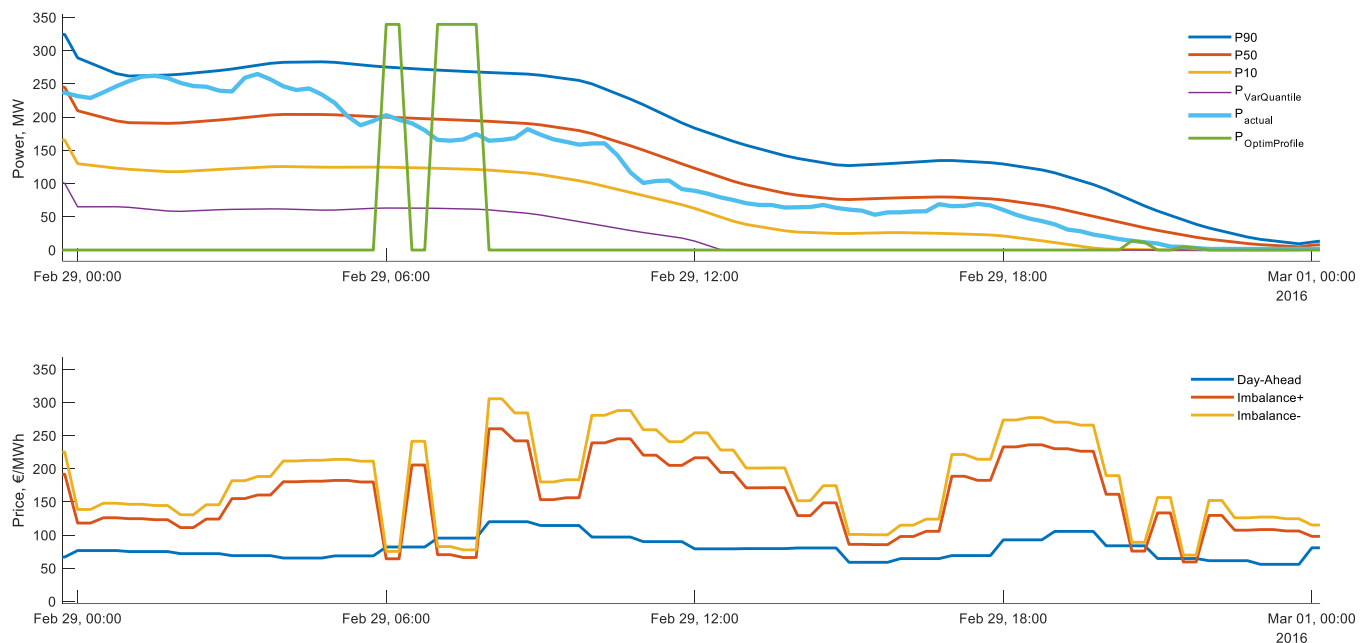


Figure 14 Example of the day when DA prices were below the imbalance prices.

Note that up to 06:00, $P_{OptimProfile}$ strategy (the green line) suggests a zero power commitment at the DA market. This is because it is more beneficial to sell all actually-generated energy at the imbalance+ price which is much higher than the DA price at this period. However, as the DA price becomes higher during other intervals (e.g. around 06:00 and 07:00), it is more beneficial to sell the energy at the DA market. Hence, we see two troughs on the green line during the same periods. Similarly, Figure 15 shows the power profiles of $P_{OptimProfile}$ strategy in the case where the DA price is higher than the imbalance+ price. In such a case, all wind energy should be sold on the DA market even if it does not follow the actual production on delivery day (the light blue line). This is explained by the fact that the revenue from high DA prices will exceed the losses due to imbalance costs. Therefore, we see that the green line is almost always equal to the installed capacity of a non-overplanted OWF (339 MW). There are also days when the DA price is located between the positive and negative imbalance prices.

As a result, the $P_{OptimProfile}$ strategy shows that there is a significant theoretical potential (up to 21%) for the revenue increase, compared to the P50 strategy. The $P_{OptimProfile}$ strategy may be exploited by market actors, provided that they get sufficiently accurate forecasts of the imbalance prices within a considerable lead time. As mentioned earlier, studies on this type of forecast are indeed emerging.

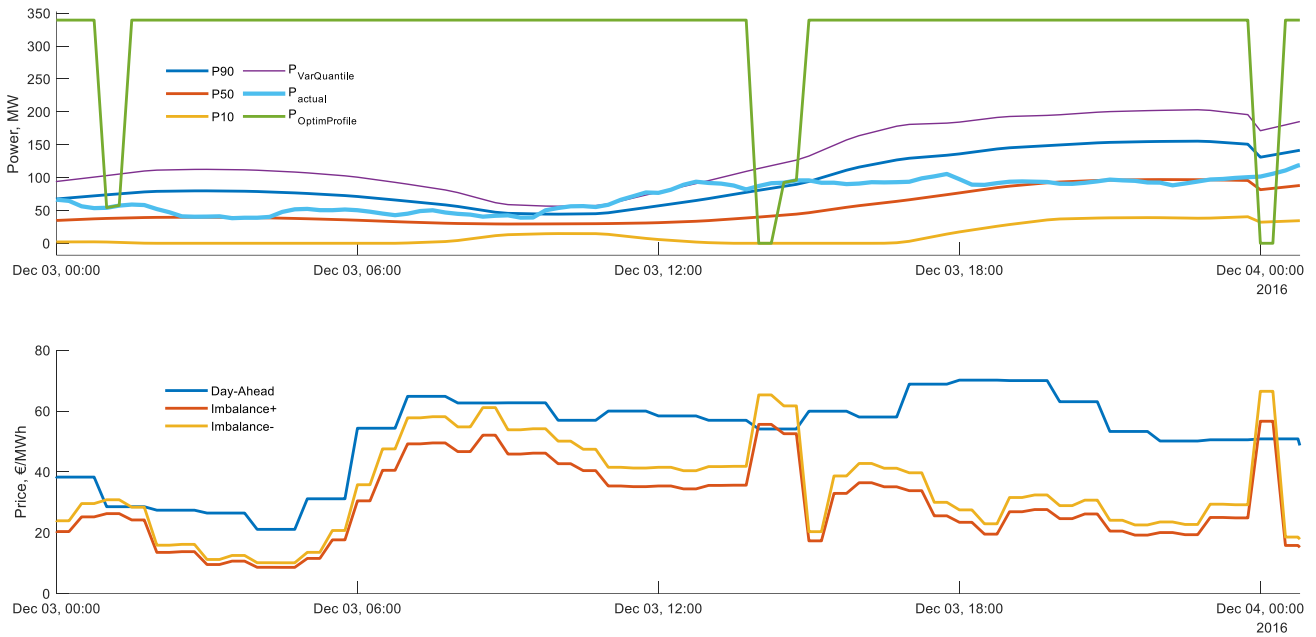


Figure 15 Example of the day when DA prices were mostly higher than the imbalance prices

In summary, adopting a fixed quantile strategy is relevant, but the problem seems to be relatively flat and quantiles other than the P50 may be adopted without a significant loss of revenue. Note, however, that this conclusion is drawn for Elia’s OWF data and may be different for other OWFs, especially under different market conditions. Moreover, improving the forecasts to commit as close as possible to the actual power profile leads to a significant, but small, revenue increase of 2 % at most. Selecting a variable quantile each day, as opposed to a constant quantile during the year, may lead to a maximum revenue increase of 5 %. Finally, it was shown that there is a large theoretical potential (up to 21%) for the revenue increase if market actors exploit the imbalance prices as well as the DA prices ($P_{OptimProfile}$ strategy). Again, this implies a sufficient level of knowledge on future energy prices with a sufficient lead time. However, it should be remarked that $P_{OptimProfile}$ strategy, although indeed it maximizes the revenue of an OWF, may complicate the TSO’s operation planning due to mismatches between the submitted OWF power profile on the DA market and the actual delivery the following day. Note also that the above-mentioned results are obtained for a not-overplanted OWF i.e. they do not consider the overplanting.

B. Impact of joint use of overplanting, DTR and commitment strategy on the revenue (Case studies 3 and 4)

In contrast to the previous section (Case study 2) where the revenue was calculated for a non-overplanted OWF, this subsection provides the results for overplanted OWFs. Specifically, Figure 16 shows how the revenue of an overplanted OWF changes as a function of the five commitment strategies. The left figure shows that the additional revenue in the case of STR varies between 0 % and 87% (i.e. 187% of the reference revenue). This range is increased up to 104% (i.e. 204% of the reference revenue) if DTR would be used as the cable limits (right figure).

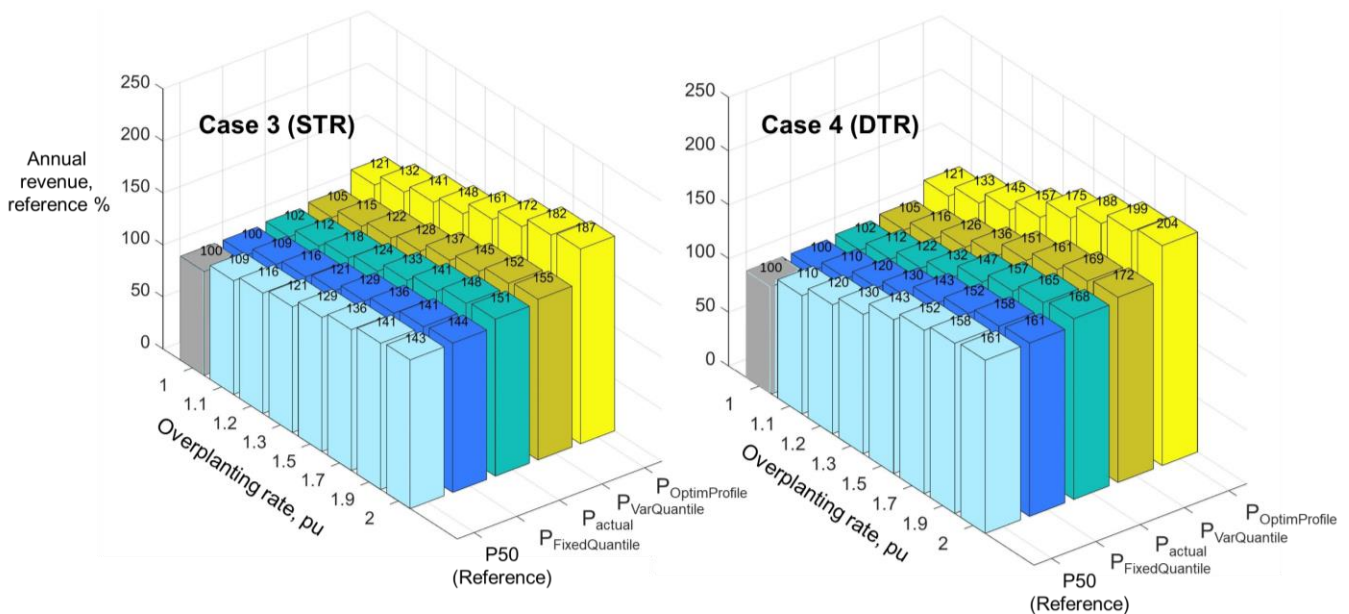


Figure 16 Annual revenue as a function of overplanting rate and commitment strategies, with STR (left) and DTR (right).

In Figure 16 and Figure 17, we see that there is no significant difference between the P50 and $P_{\text{FixedQuantile}}$ strategies regardless of the overplanting rate. In other words, there are small to negligible variations in annual revenue between all the 99 quantiles. It should be noted that the optimal quantile decreases as the overplanting rate grows (see the middle plot in Figure 17), which is explained by the increasing volume of curtailed energy. However, even though the optimal quantile is reducing down to P30, its difference with P50 in terms of annual revenue remains negligible (see the bottom plot). Once again, the problem seems to be relatively flat with respect to the quantiles, even for overplanted OWFs.

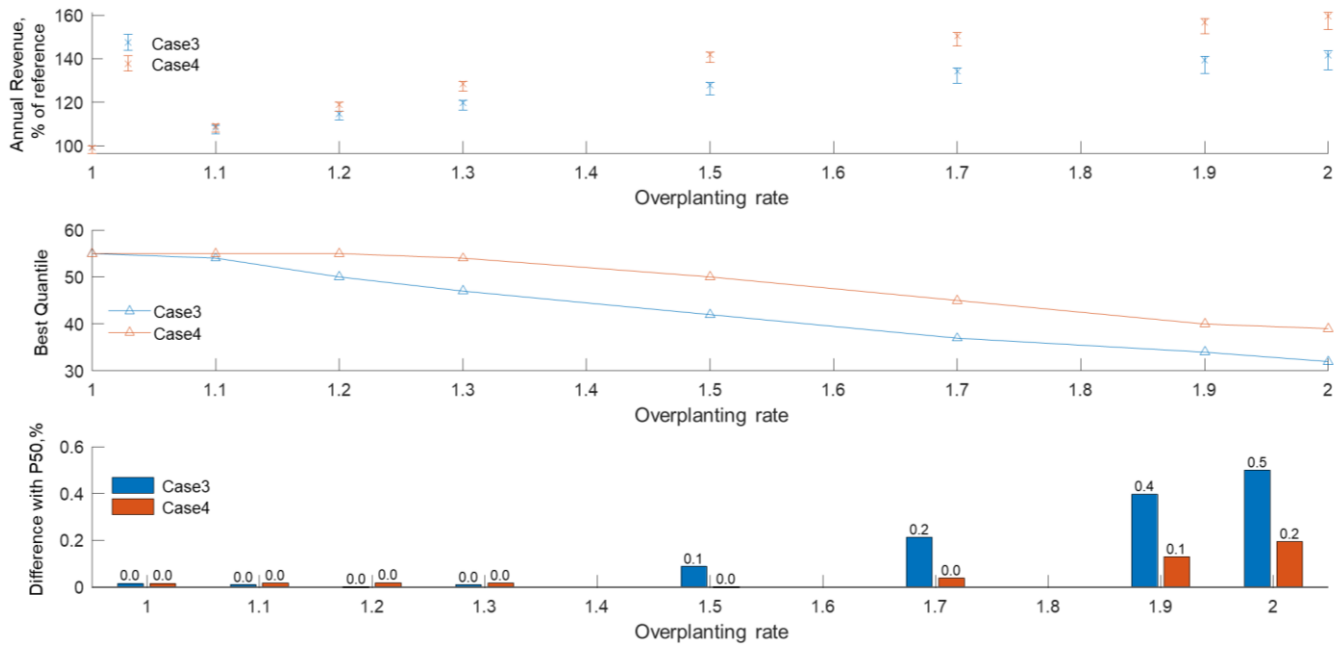


Figure 17 Annual revenue for $P_{\text{FixedQuantile}}$ (top). Best fixed quantile as a function of the overplanting rate (middle). Revenue difference between the best-fixed quantile strategy and the P50 strategy (bottom).

Going back to Figure 16, it can be observed that in the P_{actual} strategy, which is the case of an ideal forecast, the additional revenue compared to the P50 strategy increases only by 2% for a non-overplanted farm, and is limited to 7% for a farm with a theoretical overplanting rate of 200% (DTR case). On the contrary, and as already observed earlier for a non-overplanted case, the revenue increase when energy is sold as an imbalance is theoretically equal to 21% (no-overplanting) and increases with the overplanting rate. This shows that it may be more interesting economically to enhance the forecasts of the imbalance prices than in the production itself. However, this former task may be more complex than the latter.

For the STR case, it is interesting to observe the overplanting rate above which the revenue loss linked to the energy curtailment is no longer compensated by the exploitation of the energy price variability (imbalance and DA). This can be observed by comparing the increase in revenue (e.g. 175% for the variable quantile strategy with DTR) to the corresponding overplanting rate (150%). As a result, the overplanting would be economically viable up to at least 170% for the optimal profile strategy, 120% for the variable quantile strategy, and 110% if the actual power strategy was used. This shows the importance of commitment strategies on the value of the optimal overplanting rate. The same conclusion can be drawn from the results where DTR is allowed.

As for the cases with DTR (the right plot in Figure 16), it can be observed that the increase in revenue is always greater than the overplanting rate if the optimum profile strategy is used. This increase ranges between 21% when the non-overplanting option is considered and decreases slowly to 4% when an overplanting rate of 200% is considered. This means that, despite an increasing level of curtailment, which may go up to 35% when DTR is used, the revenue decrease linked to energy curtailment is more than compensated by exploiting the energy price variability. Although overplanting could remain economically viable up to at least 130% for the P50 strategy, it is shown here that with a variable quantile strategy, the minimum rate was at least equal to 150%. This drops to 130% if the fixed quantile strategy and the actual power profile strategies are used. Again, these cases are theoretical as energy prices are considered as known in advance, but it suggests that sufficient knowledge of these prices may have an important influence on the selection of an optimal overplanting rate, as well as the commitment strategies. However, defining the level of forecast quality above which this knowledge would play a significant role is out of the scope of this paper.

A sensitivity analysis was carried out regarding the maximum revenue (related to the $P_{\text{OptimProfile}}$) that could be obtained from an OWF with different overplanting rates as a function of the maximum allowed temperature (i.e. DTR is enforced here). As mentioned previously, although 90°C represents the maximum allowed temperature in XLPE-based cables, temperature monitoring devices may present a coarser precision of a few degrees. This may require curtailing the wind power at a few degrees less than 90°C. Hence, Table 3 describes the loss of revenue as a function of the maximum allowed temperature normalised to the revenue obtained when the 90°C limit is enforced. Although it is expected that temperature monitoring devices

would have an accuracy of a few degrees up to 5°C, the results for a temperature limit of 80°C are also presented for the sake of illustration. It can be observed that, when an 88°C or 85°C temperature limit is adopted, the revenue loss is small to negligible, not exceeding 2% for the ideal case of a 2 pu-overplanted farm, while a more realistic case of a 1.5-pu overplanted farm leads to a revenue loss around 1% only. Hence, in this paper, only a temperature limit of 90°C was considered.

Table 3 – Sensitivity analysis on the maximum revenue ($P_{OptimProfile}$) as a function of the maximum allowed temperature

Optimal revenue difference with the 90°C limit		Overplanting rate		
		1 pu	1.5 pu	2 pu
Temperature limit of export cable	80°C	0.0%	-2.6%	-3.4%
	85°C	0.0%	-1.2%	-1.6%
	88°C	0.0%	-0.5%	-0.6%

C. Analysis of LCOE, NPV and payback periods

This section complements the revenue analysis by evaluating such metrics as NPV, LCOE and payback periods of overplanted OWF with DTR or STR. Figure 18 shows the LCOE as a function of overplanting rate for DTR and STR. Compared to the non-overplanting case, the overplanting with both DTR and STR allows reducing the LCOE down to 1 €/MWh and 0.1 €/MWh correspondingly. Any increase beyond these optimal overplanting rates (1.1 pu for STR and 1.3 pu for DTR) leads to a significant increase in LCOE.

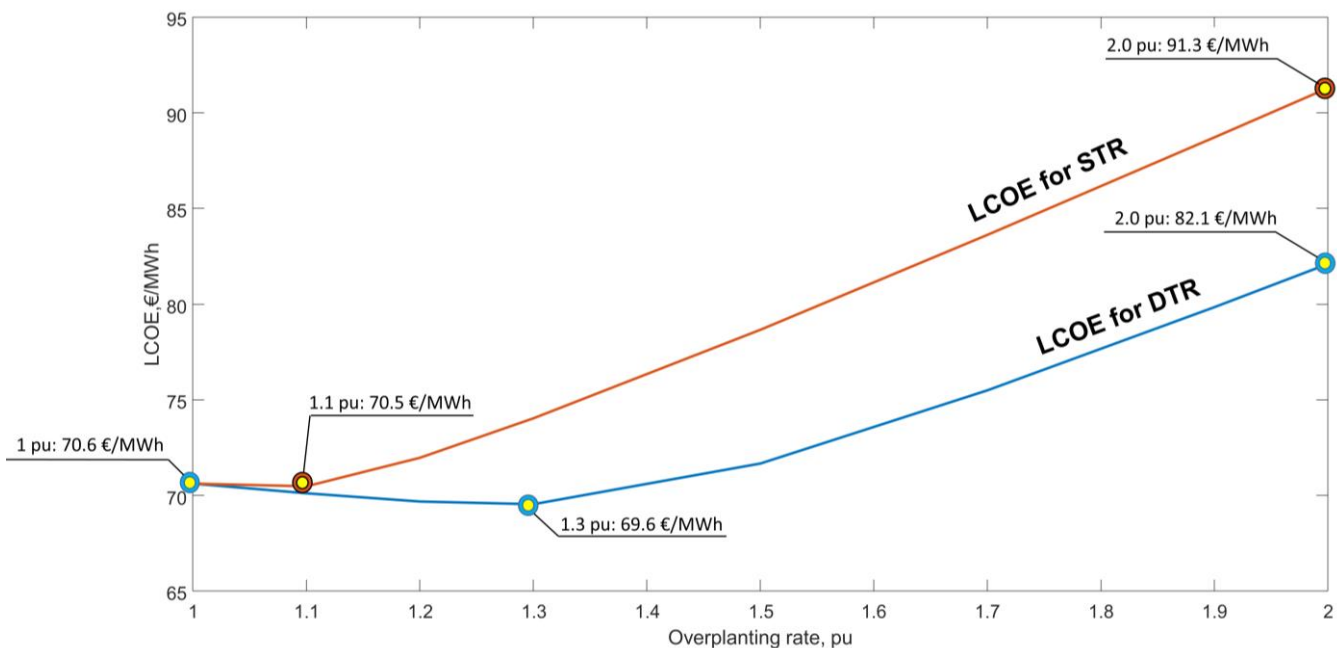


Figure 18 LCOE as a function of the overplanting rate

As the overplanting rate grows in Figure 18, the LCOE difference between STR and DTR becomes more and more evident and reaches almost 10 €/MWh for the final overplanting rate 2 pu. The difference between STR and DTR along the range of overplanting rates is explained by the lower amount of wind curtailments thanks to the full exploitation of the cable's transfer capacity by DTR. As almost no wind curtailment occurs before 1.3 pu for DTR, the optimal overplanting rate is then shifted to 1.3 pu. Although from an LCOE perspective, it may seem necessary to select an overplanting rate of 1.1 pu for the STR case and 1.3 pu for the DTR case as optimal overplanting rates, it may be not so evident which overplanting rates are optimal from the NPV perspective, as described below.

As the first part, a NPV analysis was conducted for market prices in France corresponding to 2018, which was before the global COVID outbreak and the ongoing energy crisis due to the war in Ukraine. At that time, the mean average day-ahead price in France was 51 €/MWh as well as imbalance prices were around 47-55 €/MWh. One may notice that these prices are already below LCOE (e.g. 69.6 €/MWh) obtained earlier in Figure 18. In other words, the market price at that time was below the minimum energy price needed to recover capital and operation expenditures over the lifetime of the studied OWF. Note also that capacity factors of the OWF reduce from 37% down to 30% as the overplanting rate grows. As expected for low energy prices and moderate capacity factors, NPV was negative even for the no-overplanting case (see NPV=-220 M€ in Figure 19). This means that for the studied OWF there is no incentive or a possibility to be profitable on the wholesale market (as of 2018) regardless of the overplanting rate or a commitment strategy (even the best $P_{OptimProfile}$) or increased cable capacities thanks to DTR. Graphically, this can be seen in Figure 19 as all bold lines, corresponding to various commitment strategies, reduce along the overplanting rates regardless of STR (the top figure) or DTR (the bottom figure).

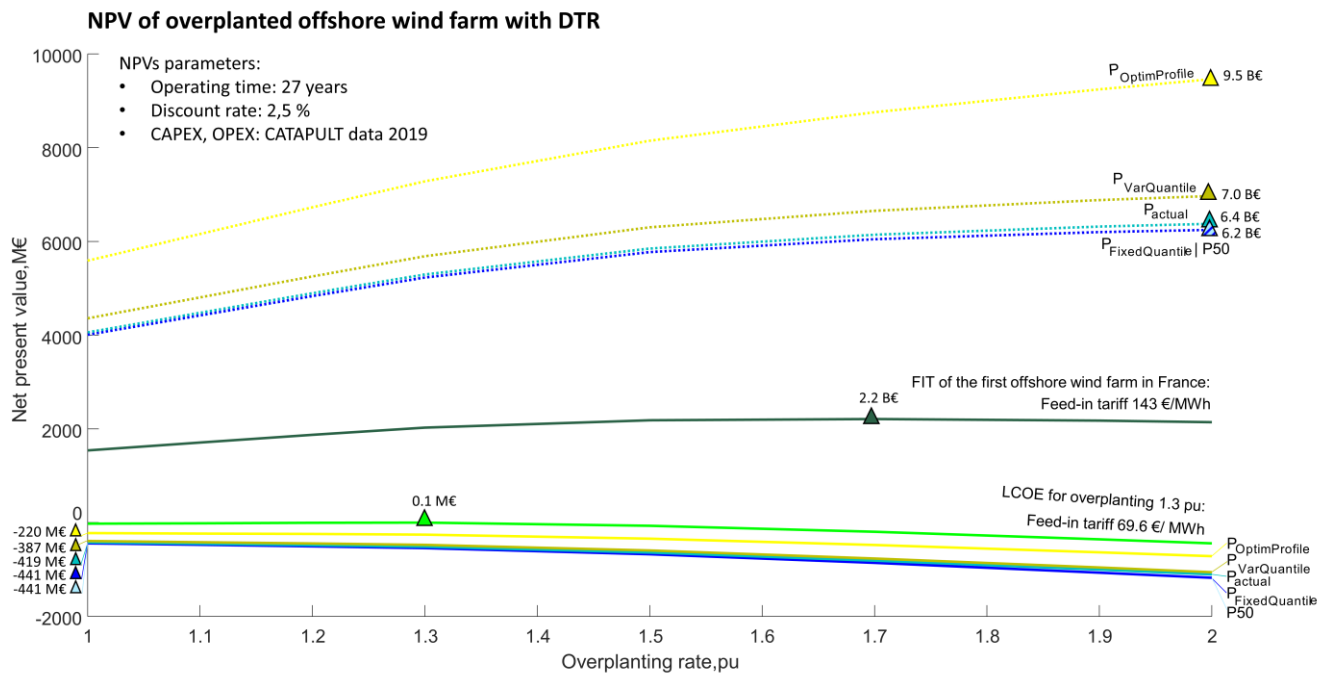
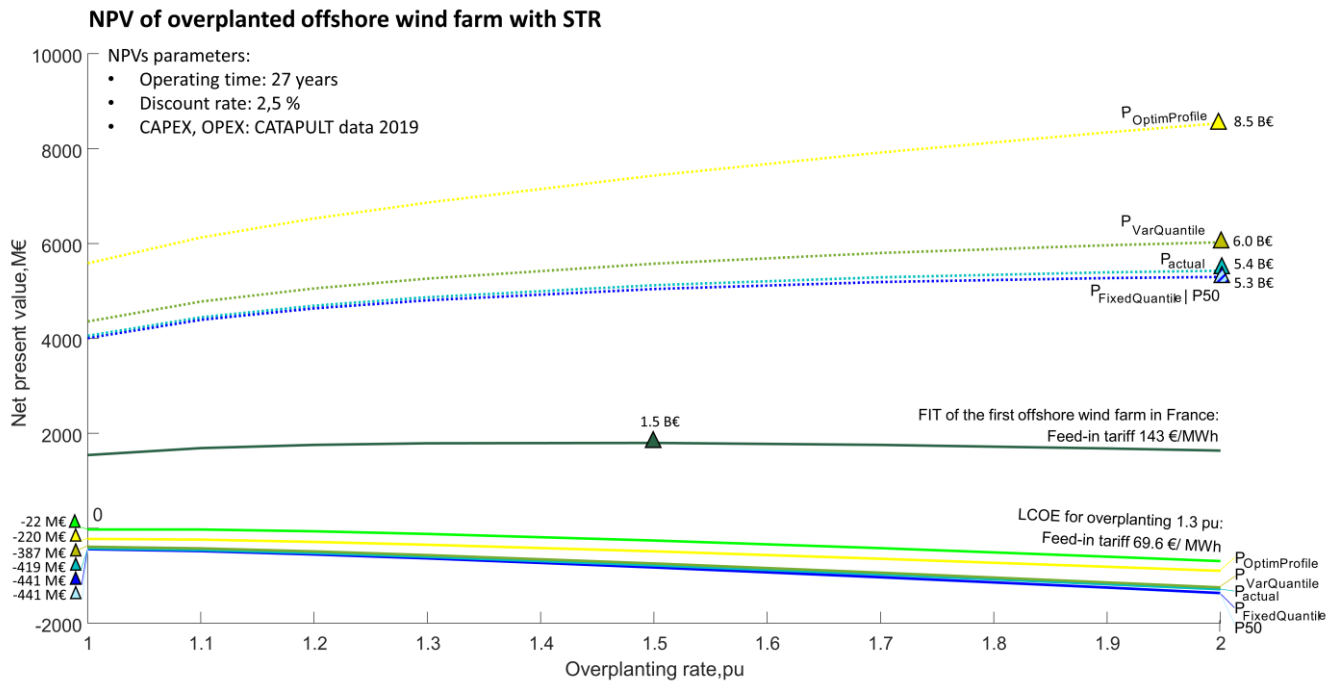


Figure 19 NPV as a function of the overplanting rate and the commitment strategy. The top figure corresponds to the case when STR is taken as a limit of export cable. The bottom figure corresponds to the case when DTR is retained as a limit of export cable. Dash lines in the upper part of each subfigure correspond to 2022 market prices while bold lines (in the lower part of each subfigure) correspond to 2018 market prices

Despite the negative NPVs at market prices of 2018, the overplanting may be profitable for the supportive mechanisms where the energy price can be set higher than the market price/ LCOE. For instance, we investigate two FITs: 69.6 €/ MWh and 143 €/ MWh. The FIT of 69.6 €/ MWh corresponds to the lowest LCOE of overplanting rate 1.3 pu (see the light green line in Figure 19). The FIT of 143 €/ MWh was taken as the industry reference as such FIT was selected for the first OWF in France (Saint-Nazaire) [108]. Note that the FIT of 143 €/ MWh is almost 3 times higher than the 2018 market price (51 €/ MWh) and 2 times higher than the LCOE of a non-overplanted OWF (70.6 €/ MWh). As a result of FITs, the corresponding NPVs become positive and for FIT of 143 €/ MWh NPV reaches from 1.5 billion € (in the case of STR) up to 2.2 billion € (in the case of DTR). These maximal NPVs are achieved at overplanting rates of 1.5 pu (STR) and 1.7 pu (DTR) which are higher than the overplanting rates ensuring the lowest LCOE (1.1 pu for STR and 1.3 pu for DTR). We believe that such a discrepancy between the optimal overplanting rates of “the lowest LCOE” and “the highest NPV” is explained by the relation between the amount of electrical energy produced and the price at which this energy is sold. To clarify this statement, the OWF, as the overplanting

rate increases, produces the same amount of energy as its lower overplanting rates plus the additional energy surplus. It seems that the economic benefits from this energy surplus may overlap (due to the high FIT) the costs of additional installed capacity and therefore shifting the optimal overplanting rate, from the NPV perspective, away from the optimal overplanting rates from the LCOE perspective. Note also that the benefit of using DTR against STR in the case of FIT (143 €/MWh) reaches 0.7 billion € (see NPV differences for dark green lines at the top and bottom of Figure 19). This benefit was not evident from LCOE calculations in Figure 18 and it seems that such high benefits advocate in the favour of DTR against STR.

Although our previous analysis showed that the overplanting was non-profitable at market prices of 2018 and profitable for FIT, it should be noted that amid the ongoing energy crisis, the market prices in 2022 increased by 5 times if compared to 2018 and even exceeded the studied FIT of 143 €/MWh. For instance, the average day-ahead price in France in 2022 was 273 €/MWh and average imbalance prices were around 255 €/MWh and 282 €/MWh. Therefore, it was decided to reconduct the NPV analysis for the market prices of 2022. As a result of this analysis, conclusions on the profitability of overplanted OWFs in the market were reversed. First, the NPV for ongoing prices is always positive and varies from 4 billion € for a non-overplanted OWF (339 MW) up to 9.5 billion € for OWF with the largest overplanting rate in our study – 2 pu (or 679 MW). The higher the overplanting rate is, the higher NPV is and the convergence to some maximal NPV values only starts appearing. Graphically, all dash lines in Figure 19, corresponding to market prices of 2022, grow as a function of overplanting rate. This means that OWF has all incentives to be profitable in the energy markets (in contrast to energy prices of 2018) and overplanting remains the feasible way to increase the profitability of an OWF. Note also that the difference between commitment strategies reaches several billion euros, e.g. 9.5 billion € for $P_{OptimProfile}$ versus 6.2 billion € for P50. This testifies to the promising incentive and motivates an OWF operator to carefully choose the commitment strategy. Moreover, the economic benefits of using DTR against STR rise to approximately 1 billion € (see NPV differences between the same strategies in Figure 19).

Note that the NPV analysis in our study is held for 27 years as CATAPULT data [107] suggests this period. Anyway, the NPV analysis does not explicitly define the year when NPV becomes positive if it becomes positive at all (in the case of the negative NPV). Therefore, Table 4 shows the discounted payback period i.e. the year when NPV becomes positive considering the time value of cash flows. Similar to NPV analysis, we estimate the payback period for energy prices before the energy crisis and COVID (B scenario) as well as after them (A scenario). For completing the analysis, payback periods of FIT mechanisms are also estimated.

Table 4 Payback periods of overplanted OWF (years)

Overplanting, pu	Commitment strategy on the day-ahead market or FIT											
	P ₅₀		P _{FixedQuantile}		P _{actual}		P _{VarQuantile}		P _{OptimalPower}		FIT 69.6	FIT 143
	B	A	B	A	B	A	B	A	B	A	€/MWh	€/MWh
DTR case												
1	101	4	101	4	86	4	71	4	41	3	28	9
1.1	96	4	96	4	82	4	69	4	41	3	28	9
1.2	92	4	92	4	80	4	68	4	40	3	28	9
1.3	92	4	92	4	79	4	67	4	40	3	27	9
1.5	145	4	145	4	103	4	82	4	43	3	29	9
1.7	Inf	5	Inf	5	Inf	5	157	4	50	4	34	9
1.9	Inf	5	Inf	5	Inf	5	Inf	5	62	4	39	10
2	Inf	5	Inf	5	Inf	5	Inf	5	70	4	43	11
STR case												
1	101	4	101	4	86	4	71	4	41	3	28	9
1.1	101	4	101	4	86	4	71	4	41	3	28	9
1.2	141	4	141	4	104	4	82	4	44	3	30	9
1.3	Inf	5	Inf	5	175	5	105	4	47	4	32	9
1.5	Inf	5	Inf	5	Inf	5	Inf	5	58	4	38	10
1.7	Inf	5	Inf	5	Inf	5	Inf	5	76	4	46	11
1.9	Inf	6	Inf	6	Inf	5	Inf	5	114	4	57	12
2	Inf	6	Inf	6	Inf	6	Inf	5	194	4	65	12

B – Based on 2018 prices *before* the energy crisis and COVID: the average day-ahead price is 51 €/MWh
A – Based on energy 2022 prices i.e. “*after*” the energy crisis: the average day-ahead price is 273 €/MWh
FIT 69.6 €/MWh – Feed-in tariff corresponding to the lowest LCOE (the overplanting 1.3 pu with DTR)
FIT 143 €/MWh – Feed-in tariff of the first offshore wind farm in France (Saint-Nazaire)

First of all, we see that for market prices of 2018 (i.e. before the energy crisis and COVID), the NPV will become positive only if an OWF would operate for around a century which is far beyond the operating time of OWF. However, even if OWF could operate for 100 years, some investments in overplanting would still never be paid back (see Inf symbols in Table 4). This is because the discounted cash flow at such long periods will become zero (due to a discount rate of 2.5 %) and therefore making the payback time to be infinite. Nevertheless, this analysis allows us to make two observations. The first observation is that the

payback period as a function of overplanting rate seems to be convex. For instance, the minimum payback period for the P_{actual} strategy occurs for the overplanting rates around 1.3 pu (which at the same time is the overplanting rate corresponding to the lowest LCOE). The second observation is that commitment strategies may have a significant impact on the payback period. For instance, $P_{\text{OptimProfile}}$ strategy allows reducing the payback time for the non-overplanted OWF from 101 years down to 41 years, which is still higher than the usual operating time of an OWF but this is much closer to realistic time intervals. Note that these results correspond to market prices which are lower than LCOE so it is expected to have such long payback times in the context of low energy prices. Concerning the context of high energy prices, we can see that the payback period varies between 3 and 6 years. Note that FIT of 143 €/MWh ensures a payback period of 9-11 years, which seems to be a reasonable payback time. Hence, the remaining operating time of up to 27 years would let the OWF generate profits.

V. CONCLUSION

The results of this paper allow us to formulate several conclusions on the annual revenue of overplanted OWFs and their profitability over their lifetime.

Concerning the annual revenue of OWF, it was observed that the annual revenue is relatively insensitive to the selected quantile of power forecast. This confirms that the business-as-usual quantile – P50 - is a good option for trading on the day-ahead market if OWF operators prefer to use the same quantile-based strategy over the year. At the same time, the P50 or best-fixed quantile strategies earn the lowest revenues in our case study. To further increase revenues, an OWF operator may adjust the quantile of the power forecast on a daily basis (instead of fixing it for the whole year). This, as it turned out, may be an even better strategy than using an ideal power forecast, which will perfectly match a committed power profile with the future (actual) power profile. Such a non-evident difference is explained by the possibility for quantile-based strategies to generate additional profits from imbalance prices compared to the strategy based on the ideal forecast that does not cause any imbalances at all. Therefore, the strategy based on the actual power profile cannot earn profits from imbalance prices which are sometimes higher than the day-ahead prices. Note, however, that the additional profit would be limited to the shape of a quantile-based power profile. If we assume that the OWF could submit any shape of power profile (not only wind-power profile based on a quantile), then such a strategy (corresponding to $P_{\text{OptimProfile}}$) could ensure the highest-possible revenue that may be taken from day-ahead and imbalance prices. Although such a strategy remains a theoretical one, it allows us to estimate the highest-possible revenue that the OWF may obtain from the given market prices.

Concerning the profitability of the OWF, it was confirmed that the final profitability of an overplanted OWF significantly depends on market prices. For the market prices before the energy crisis, the NPV of an overplanted OWF remains always negative despite positive benefits from overplanting, DTR or commitment strategy. This is simply explained by the fact that the average market price at that time was lower than the LCOE of OWF. Therefore, the least-losing approach under such low prices (and moderate capacity factors) was actually to not overplant the OWF at all. However, under existing FIT levels, the overplanting of the OWF becomes profitable and reaches 1.5 – 2.2 billion euros. The corresponding optimal overplanting rates are 1.5 pu (for STR) and 1.7 pu (for DTR). This difference of 700 million euros also corresponds to the economic benefit of DTR under FIT support. Under market prices of 2022 (i.e. corresponding to the ongoing energy crisis), the economic benefit of DTR may rise up to 1 billion euros. To the best of the author’s knowledge, this is one of the highest economic benefits of DTR in relation to the NPV given in the literature. Concerning the profitability of overplanting, we observed that the high energy prices of 2022 imply the following logic: the higher is the overplanting rate, the higher is the NPV. In our case study, the highest NPV was 9.5 billion euros and it was achieved under the maximal overplanting rate of 2 pu, used in the study. The discounted payback of overplanted OWF under energy prices of 2022 varies between 3 and 6 years only. Note that market prices, before the energy crisis, would have resulted in positive NPV only after 41 years or even in never-paid-back situations. Therefore, the profitability of overplanting at low market prices was indeed questionable but with high market prices, the higher overplanting rates ensure higher profits for the OWF.

Concerning the LCOE of OWF, we found that the optimal overplanting rates from the LCOE perspective are 1.1 pu (for STR) and 1.3 pu (for DTR). These optimal rates correspond to the lowest LCOE: 70.5 €/ MWh for STR and 69.6 €/ MWh for DTR. Compared to the LCOE of a not-overplanted OWF (70.6 €/ MWh), LCOE was reduced by 0.1 €/MWh and by 1 €/MWh correspondingly. Nevertheless, the “optimal” overplanting rate from the LCOE perspective may not correspond to the “optimal” overplanting rate from the NPV perspective. For instance, the optimal overplanting rate under high market prices is 2 pu as it ensures the highest NPV. However, the overplanting rate of 2 pu is not optimal from the LCOE perspective as the corresponding LCOE becomes 20.7 €/MWh (for STR) and 9 €/MWh (for DTR) higher than the LCOE of a not-overplanted OWF. For NPV based on FIT of 143 €/MWh, the optimal overplanting rates are 1.5 pu (for STR) and 1.7 pu (for DTR) respectively. Again, the LCOE of these overplanting rates exceeds the LCOE of a not-overplanted OWF. Having such discrepancy between the LCOE and NPV perspectives, it seems that the research on optimal overplanting rate should consider both NPV and LCOE perspectives to clarify the economic performance of an OWF.

For the purpose of open science, we provide MATLAB code and data, used in this article, in associated the GitHub repository [106].

ACKNOWLEDGEMENT

This research was conducted as a part of the “CELT4Wind” project carried out within the framework of the WEAMEC, West Atlantic Marine Energy Community, and with the funding from the CARENE and the Pays de la Loire Region. All these

organizations are gratefully acknowledged. We highly appreciated the help from specialists Guillaume Rovai and Victor Le Maire from the Belgian system operator Elia for their help with the Belgian OWFs forecast and measured data. We would like to thank a lot Alexandre Godard and Laura Cordebart from French TSO for their technical assistance, recommendations and especially comments. The authors are very grateful to Ekaterina Daminova for her help with proofreading of this article. Last but not least, we would like to thank our colleagues Didier Trichet, Laurent Dupont & Guillaume Wasselynck from the IREENA lab, Nantes University, for their technical advice and recommendations during numerous meetings.

REFERENCES

- [1] R. Barthelmie, "A Brief Review of Offshore Wind Energy Activity in the 1990's," *Wind Eng.*, vol. 22, no. 6, pp. 265–273, 1998, [Online]. Available: <https://www.jstor.org/stable/43749698>.
- [2] GWEC, "Global Wind Report 2021," 2021. Accessed: Apr. 17, 2023. [Online]. Available: <https://gwec.net/global-wind-report-2021/>.
- [3] DNV GL, "Energy Transition Outlook 2019 Power Supply and Use," 2019. Accessed: Apr. 17, 2023. [Online]. Available: <https://eto.dnv.com/2019/#foreword>.
- [4] DNV GL, "Energy Transition Outlook 2020. Power Supply and Use," 2020. Accessed: Apr. 17, 2023. [Online]. Available: <https://eto.dnv.com/2020#ETO2020-top>.
- [5] European Commission, "An EU Strategy to harness the potential of offshore renewable energy for a climate neutral future," 2020. Accessed: Apr. 17, 2023. [Online]. Available: <https://eur-lex.europa.eu/legal-content/EN/TXT/PDF/?uri=CELEX:52020DC0741&from=EN>.
- [6] M. Shafiee, F. Brennan, and I. A. Espinosa, "A parametric whole life cost model for offshore wind farms," *Int. J. Life Cycle Assess.*, vol. 21, no. 7, pp. 961–975, Jul. 2016, doi: 10.1007/s11367-016-1075-z.
- [7] C. Kost, S. Shammugam, V. Fluri, D. Peper, A. Davoodi Memar, and T. Schlegl, "Levelized Cost of Electricity - Renewable Energy Technologies," 2021. Accessed: Apr. 17, 2023. [Online]. Available: <https://www.ise.fraunhofer.de/en/publications/studies/cost-of-electricity.html>.
- [8] C. McInerney and D. W. Bunn, "Optimal over installation of wind generation facilities," *Energy Econ.*, vol. 61, pp. 87–96, Jan. 2017, doi: 10.1016/j.eneco.2016.10.022.
- [9] E. B. Mora, J. Spelling, A. H. van der Weijde, and M. Berthelot, "Cost and Uncertainty in Overplanting the Design of Offshore Wind Farms," in *IAEE International Conference 2019 - Local Energy, Global Markets*, 2019, p. 18, Accessed: Apr. 17, 2023. [Online]. Available: https://symposia.gerad.ca/iaee2019/en/schedule/view_document/8291.
- [10] TKI Wind op Zee, "The Netherlands' long-term offshore wind R&D agenda," 2019. Accessed: Apr. 17, 2023. [Online]. Available: https://www.topsectorenergie.nl/sites/default/files/uploads/Wind_op_Zee/Documenten/20190930_RAP_The-Netherlands-long-term-offshore-wind-R-D-Agenda_V05-w_0.pdf.
- [11] K. Dykes, "Optimization of Wind Farm Design for Objectives Beyond LCOE," *J. Phys. Conf. Ser.*, vol. 1618, no. 4, p. 042039, Sep. 2020, doi: 10.1088/1742-6596/1618/4/042039.
- [12] Tennet, "Position paper. Overplanting," 2015. Accessed: Jan. 14, 2022. [Online]. Available: https://www.tennet.eu/fileadmin/user_upload/Our_Grid/Offshore_Netherlands/Consultatie_proces_net_op_zee/Technical_Topics/50_ONL_15-083-T11_Overplanting_PP_v2.pdf.
- [13] M. A. H. Colin and J. A. Pilgrim, "Cable Thermal Risk Estimation for Overplanted Wind Farms," *IEEE Trans. Power Deliv.*, vol. 35, no. 2, pp. 609–617, Apr. 2020, doi: 10.1109/TPWRD.2019.2917789.
- [14] C. Wolter, H. Klinge Jacobsen, L. Zeni, G. Rogdakis, and N. A. Cutululis, "Overplanting in offshore wind power plants in different regulatory regimes," *WIREs Energy Environ.*, vol. 9, no. 3, pp. 1–16, May 2020, doi: 10.1002/wene.371.
- [15] E. B. Mora, J. Spelling, and A. H. van der Weijde, "How does risk aversion shape overplanting in the design of offshore wind farms?," *J. Phys. Conf. Ser.*, vol. 1356, no. 1, p. 012026, Oct. 2019, doi: 10.1088/1742-6596/1356/1/012026.
- [16] TenneT, "TSO Overplanting-version: Hollandse Kust (zuid) v2," 2018. Accessed: Jan. 14, 2022. [Online]. Available: https://www.tennet.eu/fileadmin/user_upload/Our_Grid/Offshore_Netherlands/ONL-TTB-04761v2_-_Overplanting_-_version_HKZ.pdf.
- [17] A. Henderson, N. Baldock, H. Yendole, G. Parker, and G. P. Greig, "Money does grow on turbines – overplanting offshore wind farms," in *Proceedings of the Global Offshore Wind Conference*, 2014, pp. 11–12.
- [18] P. Chen and T. Thiringer, "Analysis of Energy Curtailment and Capacity Overinstallation to Maximize Wind Turbine Profit Considering Electricity Price–Wind Correlation," *IEEE Trans. Sustain. Energy*, vol. 8, no. 4, pp. 1406–1414, Oct. 2017, doi: 10.1109/TSTE.2017.2682820.
- [19] C. M. McInerney and D. W. Bunn, "Optimal Oversizing of Wind Generation Facilities," *SSRN Electron. J.*, p. 41, Mar. 2015, doi: 10.2139/ssrn.2576307.
- [20] B. Elliston and I. MacGill, "Strategies to reduce grid integration costs of solar electric plants in the Australian national electricity market," in *SolarPaces Conference*, 2011, p. 8, Accessed: Apr. 17, 2023. [Online]. Available: <https://citeseerx.ist.psu.edu/viewdoc/download?doi=10.1.1.666.7320&rep=rep1&type=pdf>.
- [21] A. J. Cavallo, "High Capacity Factor Wind Turbine-Transmission Systems," in *Proceedings of the 13th Wind Energy Symposium, Energy Sources Technology Conference*, 1994, pp. 87–94.
- [22] A. J. Cavallo, "Wind energy: Current status and future prospects," *Sci. Glob. Secur.*, vol. 4, no. 1, pp. 65–109, Aug. 1993, doi: 10.1080/08929889308426393.
- [23] A. J. Cavallo, "High-Capacity Factor Wind Energy Systems," *J. Sol. Energy Eng.*, vol. 117, no. 2, pp. 137–143, May 1995, doi: 10.1115/1.2870843.
- [24] A. J. Cavallo, "Wind Tubine Cost of Electricity and Capacity Factor," *J. Sol. Energy Eng.*, vol. 119, no. 4, pp. 312–314, Nov. 1997, doi: 10.1115/1.2888038.

- [25] P. M. Silva Ferreira, "Avaliação da complementaridade dos recursos eólico e solar PV , em Portugal," Universidade de Lisboa, 2021.
- [26] L. Petersen *et al.*, "Vestas Power Plant Solutions Integrating Wind, Solar PV and Energy Storage," in *3rd International Hybrid Power Systems Workshop*, 2018, no. May, pp. 2–9, Accessed: Apr. 17, 2023. [Online]. Available: <https://vbn.aau.dk/en/publications/vestas-power-plant-solutions-integrating-wind-solar-pv-and-energy>.
- [27] IEA Wind and VTT, "Design and operation of energy systems with large amounts of variable generation," 2021. Accessed: Apr. 17, 2023. [Online]. Available: <https://cris.vtt.fi/en/publications/design-and-operation-of-energy-systems-with-large-amounts-of-vari>.
- [28] A. I. Estanqueiro, J. M. F. de Jesus, J. Ricardo, A. dos Santos, and J. A. P. Lopes, "Barriers (and Solutions...) to Very High Wind Penetration in Power Systems," in *2007 IEEE Power Engineering Society General Meeting*, Jun. 2007, pp. 1–7, doi: 10.1109/PES.2007.385802.
- [29] M. Perez, R. Perez, K. R. Rábago, and M. Putnam, "Overbuilding & curtailment: The cost-effective enablers of firm PV generation," *Sol. Energy*, vol. 180, no. December 2018, pp. 412–422, Mar. 2019, doi: 10.1016/j.solener.2018.12.074.
- [30] R. Getreuer, "Preferred offshore power grids for wind energy," Delft university, 2015.
- [31] R. E. Getreuer, B. W. Tuinema, J. L. Rueda, and M. A. M. M. van der Meijden, "Multi-parameter approach for the selection of preferred offshore power grids for wind energy," in *2016 IEEE International Energy Conference (ENERGYCON)*, Apr. 2016, pp. 1–6, doi: 10.1109/ENERGYCON.2016.7514124.
- [32] L. D. D. Harvey, "The potential of wind energy to largely displace existing Canadian fossil fuel and nuclear electricity generation," *Energy*, vol. 50, no. 1, pp. 93–102, Feb. 2013, doi: 10.1016/j.energy.2012.12.008.
- [33] N. Citroen, O. Mohammed, and M. Mohamed, "Optimization of 33/225 KV Power evacuation transformers in onshore wind farms in Morocco," in *2014 International Renewable and Sustainable Energy Conference (IRSEC)*, Oct. 2014, pp. 890–894, doi: 10.1109/IRSEC.2014.7059754.
- [34] N. Boerema and I. Macgill, "The economics of transmission constraints on wind farms – some evidence from South Australia," 2010. Accessed: Apr. 17, 2023. [Online]. Available: https://ageconsearch.umn.edu/record/107741/files/EERH_RR89.pdf.
- [35] Á. A. B. Rújula, J. M. Amada, and J. S. Arasanz, "Improving the electrical value of Wind Power Plants," in *European Wind Energy Conference & Exhibition*, 2003, p. 6, Accessed: Apr. 17, 2023. [Online]. Available: <http://citeseerx.ist.psu.edu/viewdoc/download?doi=10.1.1.77.9677&rep=rep1&type=pdf>.
- [36] D. J. Lew, "Alternatives to coal and candles: wind power in China," *Energy Policy*, vol. 28, no. 4, pp. 271–286, Apr. 2000, doi: 10.1016/S0301-4215(99)00077-4.
- [37] A. Kies, B. U. Schyska, and L. von Bremen, "The optimal share of wave power in a highly renewable power system on the Iberian Peninsula," *Energy Reports*, vol. 2, pp. 221–228, Nov. 2016, doi: 10.1016/j.egyr.2016.09.002.
- [38] C. Mushwana and H. Ganal, "Combined wind and solar feed-in to the grid," in *African utility week*, 2018, p. 30, Accessed: Apr. 17, 2023. [Online]. Available: https://researchspace.csir.co.za/dspace/bitstream/handle/10204/10248/Mushwana_20945_2018.pdf?sequence=1&isAllowed=y.
- [39] D. Vázquez Pombo *et al.*, "The First Utility Scale Hybrid Plant in Europe: The Case of Haringvliet," in *5th International Hybrid Power Systems Workshop*, 2021, no. May, pp. 1–6, Accessed: Apr. 17, 2023. [Online]. Available: https://orbit.dtu.dk/files/246852885/6A_2_HYB21_017_paper_Raducu_George_Alin_1_.pdf.
- [40] IEA Wind TCP, "Results of IEA Wind TCP workshop on a grand vision for wind energy technology," 2019. Accessed: Apr. 17, 2023. [Online]. Available: <https://ntnuopen.ntnu.no/ntnu-xmlui/handle/11250/2596867>.
- [41] D. J. Lew, R. H. Williams, X. Shaoxiong, and Z. Shihui, "Large-scale baseload wind power in China," *Nat. Resour. Forum*, vol. 22, no. 3, pp. 165–184, Aug. 1998, doi: 10.1111/j.1477-8947.1998.tb00726.x.
- [42] B. Vos, "Low-Wind Turbines in the Dutch Power," Delft University of Technology, 2021.
- [43] R. Bove, M. Bucher, and F. Ferretti, "Integrating large shares of wind energy in macro-economical cost-effective way," *Energy*, vol. 43, no. 1, pp. 438–447, Jul. 2012, doi: 10.1016/j.energy.2012.03.061.
- [44] Á. A. Bayod-Rújula, M. E. Haro-Larrodé, and A. Martínez-Gracia, "Sizing criteria of hybrid photovoltaic–wind systems with battery storage and self-consumption considering interaction with the grid," *Sol. Energy*, vol. 98, no. PC, pp. 582–591, Dec. 2013, doi: 10.1016/j.solener.2013.10.023.
- [45] J. Jurasz, B. Ceran, and A. Orłowska, "Component degradation in small-scale off-grid PV-battery systems operation in terms of reliability, environmental impact and economic performance," *Sustain. Energy Technol. Assessments*, vol. 38, no. October 2019, p. 100647, Apr. 2020, doi: 10.1016/j.seta.2020.100647.
- [46] N. Goni, J. Sacristan, A. Berrueta, J. L. Rodriguez, A. Ursua, and P. Sanchis, "New design alternatives for a hybrid photovoltaic and doubly-fed induction wind plant to augment grid penetration of renewable energy," in *2021 IEEE International Conference on Environment and Electrical Engineering and 2021 IEEE Industrial and Commercial Power Systems Europe (EEEIC / I&CPS Europe)*, Sep. 2021, pp. 1–6, doi: 10.1109/EEEIC/ICPSEurope51590.2021.9584546.
- [47] R. B. M. Ali, "Optimal generation expansion planning for electric power systems," Imperial College of Science and Technology, 1977.
- [48] J. Dujardin, A. Kahl, B. Kruyt, S. Bartlett, and M. Lehning, "Interplay between photovoltaic, wind energy and storage hydropower in a fully renewable Switzerland," *Energy*, vol. 135, pp. 513–525, Sep. 2017, doi: 10.1016/j.energy.2017.06.092.
- [49] M. H. Ali Khan *et al.*, "Designing optimal integrated electricity supply configurations for renewable hydrogen generation in Australia," *iScience*, vol. 24, no. 6, p. 102539, Jun. 2021, doi: 10.1016/j.isci.2021.102539.
- [50] A. Dutton *et al.*, "Experience in the design, sizing, economics, and implementation of autonomous wind-powered hydrogen production systems," *Int. J. Hydrogen Energy*, vol. 25, no. 8, pp. 705–722, Aug. 2000, doi: 10.1016/S0360-3199(99)00098-1.
- [51] J. G. García Clúa, R. J. Mantz, and H. De Battista, "Optimal sizing of a grid-assisted wind-hydrogen system," *Energy Convers. Manag.*, vol. 166, no. January, pp. 402–408, Jun. 2018, doi: 10.1016/j.enconman.2018.04.047.
- [52] D. Palmer, E. Koubli, T. Betts, and R. Gottschalg, "The UK Solar Farm Fleet: A Challenge for the National Grid? †," *Energies*, vol. 10, no. 8, p. 1220, Aug. 2017, doi: 10.3390/en10081220.

- [53] J. Fiorelli and M. Zuercher-Martinson, "How oversizing your array-to-inverter ratio can improve solar-power system performance," *Sol. Power World*, vol. 7, pp. 42–46, 2013, Accessed: Dec. 29, 2021. [Online]. Available: https://www.solectria.com/site/assets/files/1472/solectria_oversizing_your_array_july2013.pdf.
- [54] H. G. Beyer, "Options to Define 'Design Years' to be Used for Sizing Highly Wind Power Based Supply Systems," in *Virtual 19th Wind Integration Workshop*, 2020, p. 3, Accessed: Apr. 17, 2023. [Online]. Available: https://www.researchgate.net/profile/Hans-Georg-Beyer/publication/345764562_Options_to_Define_Design_Years_to_be_Used_for_Sizing_Highly_Wind_Power_Based_Supply_Systems/links/5fa d1622a6fdcc9389ab4dfe/Options-to-Define-Design-Years-to-be-Used-for-Sizing-Hig.
- [55] A. Dalla Riva, A. Pasquali, J. Hethy, A. Kofoed-Wiuff, M. Baldini, and J. M. Estebarez, "Potential of Smart Renewable Hubs Including Concentrated Solar Power in the Interconnected European Power System," in *IEA SHC International Conference on Solar Heating and Cooling for Buildings and Industry*, 2019, pp. 1–11, doi: 10.18086/swc.2019.29.03.
- [56] R. Thota, "Assessing the ramping behavior and system impact of wind-based hybrid power plants," Delft University of Technology, 2021.
- [57] C. M. Roselló Abad, "Collection system optimization for hybrid power plants," DTU, 2021.
- [58] A. A. Solomon, D. Faiman, and G. Meron, "Grid matching of large-scale wind energy conversion systems, alone and in tandem with large-scale photovoltaic systems: An Israeli case study," *Energy Policy*, vol. 38, no. 11, pp. 7070–7081, Nov. 2010, doi: 10.1016/j.enpol.2010.07.026.
- [59] A. Couto and A. Estanqueiro, "Assessment of wind and solar PV local complementarity for the hybridization of the wind power plants installed in Portugal," *J. Clean. Prod.*, vol. 319, no. April, p. 128728, Oct. 2021, doi: 10.1016/j.jclepro.2021.128728.
- [60] K. Das, A. D. Hansen, D. Vangari, M. Koivisto, P. E. Sørensen, and M. Altin, "Enhanced Features of Wind-Based Hybrid Power Plants," in *4th International Hybrid Power Systems Workshop*, 2019, p. 6, [Online]. Available: https://www.researchgate.net/profile/Kaushik-Das-13/publication/338173893_Enhanced_Features_of_Wind-Based_Hybrid_Power_Plants/links/5e04baf92851c83649b774b/Enhanced-Features-of-Wind-Based-Hybrid-Power-Plants.pdf.
- [61] National Grid, "The Crown Estate - Round 3 Offshore Wind Farm Connection Study," 2008. [Online]. Available: <https://www.waveandtidalknowledgenetwork.com/wp-content/uploads/legacy-files/00883.pdf>.
- [62] D. Flood, "Round 3 offshore wind farms UK Future Energy Scenarios seminar 2012," 2012. Accessed: Dec. 09, 2021. [Online]. Available: <https://www.nationalgrideso.com/sites/eso/files/documents/davidfloodround3windfarms.pdf>.
- [63] B. O. Donovan, "Connection Offer Policy & Process (COPP)," 2011. Accessed: Nov. 12, 2020. [Online]. Available: <https://www.cru.ie/wp-content/uploads/2016/07/CER11093-Connection-Offer-Policy-and-Process.pdf>.
- [64] N. Morris, "Decision on Installed Capacity Cap," 2014. Accessed: Nov. 12, 2020. [Online]. Available: <https://www.cru.ie/wp-content/uploads/2014/07/CER14047-Decision-Paper-COPP-Installed-Capacity-Cap.pdf>.
- [65] DNV GL, "Sharing Lessons Learned and Good Practice in Offshore Transmission A Report for The Crown Estate," 2014. Accessed: Apr. 17, 2023. [Online]. Available: <https://citeseerx.ist.psu.edu/viewdoc/download?doi=10.1.1.736.9909&rep=rep1&type=pdf>.
- [66] The Crown Estate, "Sharing lessons learned and good practice in offshore transmission," 2014. Accessed: Nov. 13, 2020. [Online]. Available: <https://www.offshorewindscotland.org.uk/media/1005/ei-sharing-lessons-learned-and-good-practice-in-offshore-transmission-summary.pdf>.
- [67] A. Henderson, N. Baldock, I. A. Aristi, and C. Newton, "Low-hanging Fruit for Reducing the Cost of Energy Optimising the Electrical Export Capacity," in *Proceedings of European Offshore Wind*, 2015, no. March, p. 23, Accessed: Apr. 17, 2023. [Online]. Available: <http://www.ewea.org/offshore2015/conference/allposters/PO206.pdf>.
- [68] E. B. Mora, "Cost and Uncertainty in Overplanting the Design of Offshore Wind Farms," The University of Edinburgh, 2020.
- [69] A. R. Silva and A. Estanqueiro, "From Wind to Hybrid: A Contribution to the Optimal Design of Utility-Scale Hybrid Power Plants," *Energies*, vol. 15, no. 7, p. 2560, Apr. 2022, doi: 10.3390/en15072560.
- [70] CIGRE WG B1.35, "A guide for rating calculations of insulated power cables," 2015. Accessed: Apr. 17, 2023. [Online]. Available: <https://e-cigre.org/publication/640-a-guide-for-rating-calculations-of-insulated-cables>.
- [71] IEC, "60287-1-1 Electric cables – Calculation of the current rating – Part 1-1: Current rating equations (100 % load factor) and calculation of losses," Geneva, 2006. Accessed: Apr. 17, 2023. [Online]. Available: <https://webstore.iec.ch/publication/1266>.
- [72] IEC, "60287-2-1 Electric cables – Calculation of the current rating – Part 2-1: Thermal resistance – Calculation of thermal resistance," 2006. Accessed: Apr. 17, 2023. [Online]. Available: <https://webstore.iec.ch/publication/22254>.
- [73] T. Kvarts, I. Arana, R. Olsen, and P. Mortensen, "Systematic description of dynamic load for cables for offshore wind farms. Method and experience," in *CIGRE Session*, 2016, p. 12, Accessed: Apr. 17, 2023. [Online]. Available: https://e-cigre.org/publication/B1-303_2016.
- [74] J. Pilgrim and S. Kelly, "Thermal and economic optimisation of windfarm export cable," *J. Eng.*, vol. 2019, no. 18, pp. 4991–4995, Jul. 2019, doi: 10.1049/joe.2018.9272.
- [75] MegaVind, "Increasing the Owners' Value of Wind Power Plants in Energy Systems with Large Shares of Wind Energy," 2014. Accessed: Apr. 17, 2023. [Online]. Available: <https://megavind.winddenmark.dk/publications/increasing-the-owners-value-of-wind-power-plants-in-energy-systems-with-large-shares>.
- [76] S. H. Hasan Kazmi, J. Holboll, T. H. Olesen, and T. S. Sorensen, "Thermoelectric Modelling and Optimization of Offshore Windfarm Export Systems - State of the Art," in *2019 1st Global Power, Energy and Communication Conference (GPECOM)*, Jun. 2019, pp. 331–336, doi: 10.1109/GPECOM.2019.8778513.
- [77] J.-A. Pérez-Rúa, K. Das, and N. A. Cutululis, "Improved Method for Calculating Power-Transfer Capability Curves of Offshore Wind Farms Cables," in *CIGRÉ Aalborg International Symposium*, 2019, pp. 1–6, Accessed: Apr. 17, 2023. [Online]. Available: <https://orbit.dtu.dk/en/publications/improved-method-for-calculating-power-transfer-capability-curves->.
- [78] D. Vree, S. Vink, J. W. Van Doeland, and F. S. W. De Vries, "Ampacity calculation method for deeply buried wind farm AC submarine export cables," in *CIGRE Session*, 2018, p. 10, Accessed: Apr. 17, 2023. [Online]. Available: https://e-cigre.org/publication/SESSION2018_B1-118.
- [79] Netherlands Enterprise Agency, "General information Borssele WFZ," 2021. <https://offshorewind.rvo.nl/generalborssele> (accessed Jan. 01, 2022).

- [80] B. H. Bulder, E. T. G. Bot, and A. J. Marina, "Scoping analysis of the potential yield of the Hollandse Kust (zuid) wind farm sites and the influence on the existing wind farms in the proximity," 2016. Accessed: Apr. 17, 2023. [Online]. Available: <https://publicaties.ecn.nl/PdfFetch.aspx?nr=ECN-E--16-021>.
- [81] B. H. Bulder, E. T. G. Bot, and E. J. Wiggeinkhuizen, "Yield assessment Wind Farm Hollandse Kust noord Scoping analysis for three different wind turbine types," 2019. Accessed: Apr. 17, 2023. [Online]. Available: <https://publications.tno.nl/publication/34634756/V0COZi/TNO-2019-R11357.pdf>.
- [82] M. A. Hernandez Colin, "Probabilistic dynamic cable rating algorithms," University of Southampton, 2020.
- [83] S. H. H. Kazmi, "Dynamic Rating based Design and Operation of Offshore Windfarm Export Systems," DTU, 2021.
- [84] N. Viafora, K. Morozovska, S. H. H. Kazmi, T. Laneryd, P. Hilber, and J. Holbøll, "Day-ahead dispatch optimization with dynamic thermal rating of transformers and overhead lines," *Electr. Power Syst. Res.*, vol. 171, pp. 194–208, Jun. 2019, doi: 10.1016/j.epsr.2019.02.026.
- [85] N. Viafora, J. Holbøll, S. H. H. Kazmi, T. H. Olesen, and T. S. Sørensen, "Load Dispatch optimization using Dynamic Rating and Optimal Lifetime Utilization of Transformers," in *2019 IEEE Milan PowerTech*, Jun. 2019, pp. 1–6, doi: 10.1109/PTC.2019.8811002.
- [86] S. H. H. Kazmi, N. Viafora, T. S. Sørensen, T. H. Olesen, B. C. Pal, and J. Holbøll, "Offshore Windfarm Design Optimization using Dynamic Rating for Transmission Components," *IEEE Trans. Power Syst.*, pp. 1–1, 2021, doi: 10.1109/TPWRS.2021.3118278.
- [87] S. H. H. Kazmi *et al.*, "Cost optimized dynamic design of offshore windfarm transformers with reliability and contingency considerations," *Int. J. Electr. Power Energy Syst.*, vol. 128, p. 106684, Jun. 2021, doi: 10.1016/j.ijepes.2020.106684.
- [88] Clean Energy Wire, "Offshore wind farm balancing German power grid seen as energy transition 'milestone.'" <https://www.cleanenergywire.org/news/offshore-wind-farm-balancing-german-power-grid-seen-energy-transition-milestone> (accessed Jun. 10, 2022).
- [89] R. Dupin, A. Michiorri, and G. Kariniotakis, "Dynamic line rating day-ahead forecasts - Cost benefit based selection of the optimal quantile," *CIREC Work. 2016*, vol. 2016, no. June, pp. 1–4, 2016, doi: 10.1049/cp.2016.0722.
- [90] P. Haessig, "Dimensionnement et gestion d'un stockage d'énergie pour l'atténuation des incertitudes de production éolienne," ENS Cachan, 2014.
- [91] Emissions-euets, "Imbalance Settlement Period (Electricity Balancing Market) - Emissions-EUETS.com," 2020. <https://www.emissions-euets.com/internal-electricity-market-glossary/603-imbalance-settlement-period> (accessed Dec. 19, 2021).
- [92] J. Lago, G. Marcjasz, B. De Schutter, and R. Weron, "Forecasting day-ahead electricity prices: A review of state-of-the-art algorithms, best practices and an open-access benchmark," *Appl. Energy*, vol. 293, p. 21, Jul. 2021, doi: 10.1016/j.apenergy.2021.116983.
- [93] T. Jónsson, P. Pinson, H. Nielsen, and H. Madsen, "Exponential Smoothing Approaches for Prediction in Real-Time Electricity Markets," *Energies*, vol. 7, no. 6, pp. 3710–3732, Jun. 2014, doi: 10.3390/en7063710.
- [94] L. Endemaño-Ventura, J. Serrano González, J. M. Roldán Fernández, M. Burgos Payán, and J. M. Riquelme Santos, "Optimal energy bidding for renewable plants: A practical application to an actual wind farm in Spain," *Renew. Energy*, vol. 175, pp. 1111–1126, Sep. 2021, doi: 10.1016/j.renene.2021.05.054.
- [95] P. Avis and J. Lee, "Evaluating System Imbalance Forecasting Models for the United Kingdom Electricity Market," 2021. <https://www.cefims.ac.uk/research/papers/DPI63/dp163.pdf> (accessed Dec. 19, 2021).
- [96] C. Contreras, "System imbalance forecasting and short-term bidding strategy to minimize imbalance costs of transacting in the spanish electricity market," Universidad Pontificia Comillas, 2016.
- [97] T. S. Salem, K. Kathuria, H. Ramampiaro, and H. Langseth, "Forecasting Intra-Hour Imbalances in Electric Power Systems," *Proc. AAAI Conf. Artif. Intell.*, vol. 33, pp. 9595–9600, Jul. 2019, doi: 10.1609/aaai.v33i01.33019595.
- [98] TenneT, "Requirements reactive power," 2015. Accessed: Jan. 14, 2022. [Online]. Available: https://www.tennet.eu/fileadmin/user_upload/Our_Grid/Offshore_Netherlands/Consultatie_proces_net_op_zeel/Technical_Topics/38_ONL_15-356_Reactive_Power_Strategy.pdf.
- [99] "Cableizer - Cable Engineering Software." <https://www.cableizer.com/> (accessed Jan. 02, 2022).
- [100] G. Liu, M. Fan, P. Wang, and M. Zheng, "Study on Reactive Power Compensation Strategies for Long Distance Submarine Cables Considering Electrothermal Coordination," *J. Mar. Sci. Eng.*, vol. 9, no. 1, p. 90, Jan. 2021, doi: 10.3390/jmse9010090.
- [101] Elia, "Wind-power generation," 2021. <https://www.elia.be/en/grid-data/power-generation/wind-power-generation> (accessed Dec. 13, 2021).
- [102] ENTSO-E, "Imbalance Prices." <https://transparency.entsoe.eu> (accessed Dec. 13, 2021).
- [103] ENTSO-E, "Day-ahead Prices." <https://transparency.entsoe.eu/> (accessed Dec. 13, 2021).
- [104] IEC, "60853-2 Calculation of the cyclic and emergency current rating of cables," 1989. [Online]. Available: <https://webstore.iec.ch/publication/3711>.
- [105] WEAMEC, "CELT4Wind Cable Electrothermal Management for Offshore Wind Farms," 2021. <https://www.weamec.fr/en/projects/celt4wind/> (accessed Dec. 24, 2021).
- [106] I. Daminov, "MATLAB code and data for the article Economic performance of overplanted offshore wind farm under several commitment strategies and dynamic thermal ratings of submarine export cable." <https://github.com/Ildar-Daminov/Economic-performance-of-overplanted-offshore-wind-farm-under-several-commitment-strategies-and-DTR> (accessed Mar. 11, 2023).
- [107] CATAPULT, "Wind farm costs – Guide to an offshore wind farm," 2019. <https://guidetoanoffshorewindfarm.com/wind-farm-costs> (accessed Feb. 28, 2023).
- [108] European Commission, "Government support for offshore wind farms in France," 2019. Accessed: Apr. 17, 2023. [Online]. Available: <https://www.actu-environnement.com/media/pdf/news-33988-decision-tarif-achat-eolien-mer.pdf>.